POLITECNICO DI MILANO

Department of Electronics, Information and Bioengineering

Master of Science in Biomedical Engineering

POLITECNICO
MILANO 1863

Haptic Virtual Reality Surgical Simulator for Training of Percutaneous Renal Access: a Feasibility Study

Advisor: Prof. Giancarlo FERRIGNO

Foreign advisor: Cristian LUCIANO, PhD.

Co-advisor: Prof.ssa Elena DE MOMI

Master Thesis of

Andrea FASO

Student ID: 852670

Academic year 2016/2017

Let's cross over.

Elizabeth Gilbert

To my family, to my friends, to the ones that I always keep in my heart, to life changing, to the good old things that remain and to the new ones that will come.

Sommario

L'accesso renale percutaneo (PCA) è una procedura chirurgica tecnicamente impegnativa che richiede una formazione approfondita e presenta una lunga curva di apprendimento. I simulatori esistenti che usano manichini e animali sono inaccurati, costosi o soggetti a una rapida degradazione dei materiali. Inoltre, il training prolungato con un vero fluoroscopio espone i tirocinanti a quantità cospicue di radiazioni, limitandone l'uso. I simulatori in realtà virtuale attualmente disponibili non forniscono feedback tattile. Poiché i medici si basano principalmente su di esso per eseguire procedure chirurgiche, l'integrazione aptica è indiscutibilmente essenziale per un simulatore realistico, insieme ad una riproduzione accurata dell'anatomia umana.

Il progetto del simulatore aptico chirurgico in realtà virtuale si concentra sullo sviluppo e la valutazione di uno strumento per il training sulla puntura renale percutanea. Mediante l'uso della tecnologia aptica in ambiente virtuale, l'applicazione consente ai tirocinanti di imparare come perforare correttamente un rene sotto guida fluoroscopica, esplorando un corpo umano virtuale 3D e sperimentando sensazioni tattili reali toccando la superficie di pelle, ossa, reni e sistema collettivo, polmoni, milza e vasi con un ago virtuale.

Il nostro innovativo VRS aptico ha mostrato il potenziale per essere una risorsa importante per migliorare l'attuale formazione degli studenti di Radiologia interventistica e Urologia, con l'obiettivo di migliorare la coordinazione occhio-mano e abbreviare la curva di apprendimento per la PCA, permettendo una preparazione estensiva in un ambiente libero da radiazioni, senza compromettere la sicurezza del paziente.

Summary

Percutaneous renal access (PCA) is a technically challenging surgical procedure that requires extensive training and presents a steep learning curve for medical residents. Current PCA simulators using manikins and animals are either inaccurate, highly priced, or subject to quick tissue degradation. Also, the prolonged training with a real fluoroscope exposes trainees to conspicuous amounts of radiation, limiting its use. Currently-available virtual reality simulators do not provide haptic feedback. Since physicians rely mainly on tactile feedbacks to execute surgical procedures, the integration of haptics is indisputably essential for a realistic simulator, along with an accurate reproduction of the human anatomy.

The haptics-based virtual reality surgical simulator project focuses upon the development and evaluation of a tool for training in percutaneous renal access. By the use of virtual reality and haptics technology, the application allows trainees to learn how to correctly puncture a kidney under fluoroscopy guidance, by exploring a 3D virtual human body and experiencing real tactile sensations while touching the surface of skin, bones, kidneys and collecting system, lungs, spleen and vessels with a virtual needle.

Our innovative haptics-based VRS the potential to be an important resource for enhancing the current training of Interventional Radiology and Urology residents, with the objective of improving their hand-eye coordination and shorten the learning curve for PCA, allowing extended training in a radiation-free environment without compromising patient safety.

Table of contents

List of figures

List of tables

List of abbreviations

API	Application programming interface
AS	Ascension
CT	Computerized tomography
DICOM	Digital Imaging and Communication in Medicine
DoF	Degrees of freedom
EMTS	Electromagnetic Tracking System
GUI	Graphical User Interface
MHD	MetaImage
MRI	Magnetic Resonance Imaging
PCA	Percutaneous renal access
PCNL	Percutaneous nephrolithotomy
QH	QuickHaptics
ROI	Region of interest
STL	StereoLithography
US	Ultrasound
UC	Urothelial carcinoma
VL	Visualization Library
VR	Virtual reality
WK	Wykobi
2D	2-dimensional
3D	3-dimensional
4D	4-dimensional

Chapter 1

1. Introduction

Obtaining percutaneous renal access (PCA) is one of the most challenging task in performing percutaneous renal surgery like percutaneous nephrolithotomy (PCNL), and it is the main determinant of the result of the procedure: while a good puncture can lead to a safe and effective clearance of the kidney, a poor access is responsible for major complications like bleeding and renal traumas.

PCA is executed by urologists and interventional radiologists, and the main issue is to mentally convert a 2D fluoroscopy image into a 3D reconstruction of the patient's anatomy to correctly reach the calix of choice. For this reason, acquiring the necessary skills to obtain a good percutaneous access to the kidney is linked to a steep learning curve. Furthermore, unlike most of other surgeries and practices in the operating room, PCA is usually done once for each procedure, and this prevents the surgeons from gaining experience and confidence in the surgery.

Hence, the need for an anatomically accurate and economically accessible preparation outside the operating room has occurred. Most of the competencies obtained by clinicians are due to situational events, but the use of simulators can accelerate training. A simulator could diminish the time associated with learning the procedure, and reduce the risks for patients as trainees start operating.

Several training models have been developed and evaluated in literature, but each one of them presents some drawbacks: current virtual simulators are expensive, *ex-vivo* animal organs are physically inaccurate and non-biological models are usually degradable, high-priced and anatomically unreliable.

Computer-based, virtual reality platforms offer the possibility to overcome limitations due to learning-by-opportunity and reproduction of human anatomy. The flexibility of the VR simulator and of its development could easily lead to patient-focused surgery preparation, targeted to a preliminary evaluation of possible drawbacks during the operation.

The aim of this research is to develop and evaluate an anatomically accurate, low-cost haptics-based virtual reality surgical simulator for training in percutaneous renal access. Kidney puncture could be accurately simulated by haptic technology, providing the clinician with accurate anatomical orientation and a step-by-step tactile feedback ideal for the acquirement of puncture skills. Being patient specific, our model could provide a reliable source of puncture planning for the inexperienced clinician, offering a cost-effective application that could be extensively used in the medical field.

This thesis is organized in seven chapters. Chapter 2 gives background information about the anatomy of the kidney and the theoretical basis for percutaneous renal surgery. It also presents an overview of the current training models for percutaneous renal puncture and haptics-based medical simulator. Chapter 3 contains the motivation, a detailed definition of the problem statement and the proposed solution. Chapter 4 shows the implementation details of the haptic and virtual reality simulator for training in percutaneous renal access. Chapter 5 outlines the experimental protocol and the results from the quantitative and qualitative assessment of the simulator. Finally, chapters 6 and 7 present and summarize the discussion and conclusions of this work and suggests future research and development.

.

Chapter 2

2. Background[1]

2.1 Anatomy of the kidney

The kidneys are paired organs which are placed within the abdominal cavity in the lumbar region. They are located posteriorly to the other bowels, behind the peritoneum, and they are symmetric with respect to the vertebral column. They are part of the urinary apparatus, whose main function is to expel waste organic substances from the body; the kidneys, in particular, separate these constituents from the blood, allowing their elimination within the urine via the urinary tracts.

The kidneys are bean-shaped structures, with smooth surface and a notch on the medial margin called hilum of the kidney. They are covered by a fibrous capsule bonded to the kidney by means of loose connective tissue. In adult subjects, the kidneys are on average 10-13 cm long, 6-8 cm wide and 2-2.5 cm thick, and they weigh 130 g. On their surface are sometimes present footprints from near organs, different for the right and the left kidney. The front face is convex, the rear almost flat; the upper pole is wide, while the lower is sharpened. Between the faces there are margins, convex the lateral, concave the medial, where vessels, nerves and pelvis are located. Deeply inside there is the renal sinus, which has the same shape of the kidney, but smaller, in which renal papillae protrude.

The renal parenchyma is organized into a deep medullary portion and an outer cortical region, partly interpenetrated. The medullary region is white, constituted by the

[1] *This chapter has been mainly taken from the work of the author at* [38].

renal pyramids (pyramids of Malpighi), whose apexes protrude into the renal sinus as renal papillae, from where the urine produced by the kidneys goes into the pelvis down through the ureters. The cortical portion has a deep red-brown color, its tissue surrounds the renal pyramids as a capsule forming the kidney columns (*pars radiata*) and spreading all over the periphery (*pars convoluta*). The kidney lobes are anatomical units consisting of the medullary pyramid and its surrounding cortical tissue.

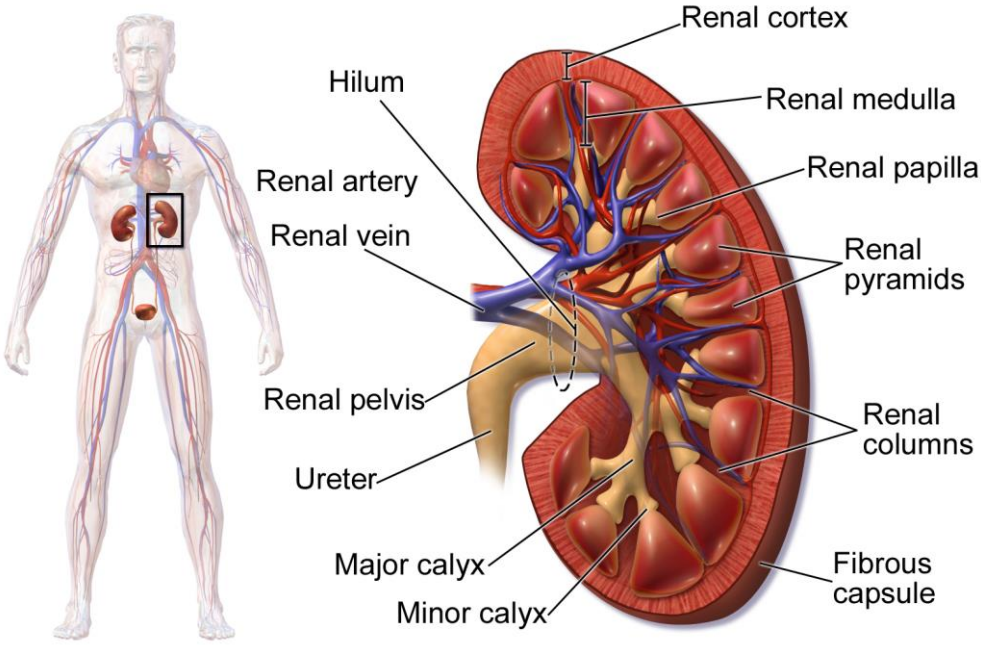

Figure 1: Anatomy and positioning of the kidney. [Reprinted with permission by https://commons.wikimedia.org/w/index.php?curid=31118599]

Approximately 20% of the cardiac output supplies the kidneys through the renal arteries, which branch from the abdominal aorta. The left and the right renal artery subdivides into five segmental arteries, that carry blood to the different districts of the kidney. Each one of them enters the hilum of the kidney and splits into the interlobar arteries, positioned between the pyramids through the renal columns and supply blood toward the external part of the organ. They then form the arcuate arteries in the spot between the cortex and medulla, which branch into the interlobular arteries. Each interlobular artery divides into afferent arterioles, which end in the glomeruli, a bunch of capillaries that filter blood to produce urine. The filtrate then reaches the collecting channels in the medullary region, which converge to the apex of the renal pyramid, the

renal papilla. Urine then accumulates in 9-13 minor calices, which end up aggregating into 3-4 major calices. Filtrate flows from the major calices into the renal pelvis, and finally propels away from the kidney through the ureters.

The right kidney is usually two to three centimetres lower than the left one for the presence of the liver: they are located between the last thoracic vertebra bodies (XII) and the first two lumbar vertebrae. The lower end of the right kidney is located 3 cm higher than the iliac crest, while the correspondent part of the left one is 5 cm higher.

The kidney relations are mediated by the renal fascia and in some tracts by the peritoneum, and they are different from right to left kidney. The adrenal gland covers the upper end. The right kidney is anteriorly related to the liver and right colon, while the left one is related to pancreas in the upper part, to stomach and spleen medially, and to left colon and mesenteric intestine in the lower end. Posteriorly, their upper third part is covered by the diaphragm, and they are located over the quadratus lumborum muscles (laterally) and the psoas (medially) [1].

2.2 Percutaneous renal surgery

A percutaneous renal access is the preliminary step for those procedures referable to percutaneous surgery for the kidney. Among those, percutaneous nephrolithotomy (PCNL) is considered the standard minimally invasive approach for the management of large-burden kidney stones.

PCNL has largely substituted open surgery to constitute the standard treatment for large and/or staghorn calculi, but it is additionally performed to treat renal stones in the lower poles and calculi in patients with atypical kidney.

Percutaneous renal access technique has evolved into a treatment option for non-invasive urothelial tumours of the upper urinary tract and adapted for the management of obstructed ureters [2].

Upper urinary tract urothelial carcinoma represents approximately 5–10% of all upper tract tumours. Although radical nephroureterectomy has historically been considered the standard treating approach, several surgical alternatives exist for dealing with upper urinary tract UC, and a percutaneous methodology is also sometimes followed [3].

Current techniques for PCA involve fluoroscopic or ultrasound guidance with a small-gauge needle for the initial puncture, with the use of computed tomography (CT) guidance for selected cases. The possible complications of a percutaneous approach are minimal, and the related morbidity is far lower than that associated with open surgery.

2.2.1 Anatomical considerations

Expertise in the basic anatomy of kidneys is crucial to obtain a safe access, and in particular of the renal vascularization in order to avoid haemorrhagic complications. Puncturing a posterior calix is usually preferred as it is simpler to handle the guide wire into the ureter, but if the pathology is spread within several calices puncturing an upper calix should be considered for easily accessing all the desired areas of the collecting system with an inflexible instrument.

The safest entry line to the collecting system is the one aligned with the infundibulum along the axis of the chosen calix: this allows the surgeon to reduce the torque of the rigid nephroscope, preventing unwanted bleeding and injury to the kidney. Direct puncture of the of the renal pelvis is excessively traumatic, as well as an infundibular perforation, and can cause significant haemorrhage [4]. The extreme part of the kidney is posterior or posterolateral to the colon, and to avoid damages to it the puncture needle should be inserted medially to the posterior axillary line. Finally, a puncture too close to ribs and a medial one should not be performed to escape the risk of injury to the intercostal nerves and to the paraspinal muscles, respectively.

2.2.2 Percutaneous renal access under fluoroscopic guidance

Percutaneous renal access could be performed under fluoroscopy, ultrasound (US) or computerized tomography guidance. Among these, bi-planar fluoroscopy is the standard imaging method for PCA. Mobile C arm units are readily available in most operating rooms. Fluoroscopy is an imaging method that shows a real time radiographic image on a screen. During the surgery, the reconstructed image deriving from the X-ray beam travelling through the patient is then sent to a monitor so that variation in the shape and the size of the areas instilled with contrast substance could be visualized in detail and the movement of the patient’s body and structures could be tracked in real time.

Initial access with fluoroscopic guidance is more challenging than with US, as soft tissues around the kidneys cannot be distinguished, therefore retrograde injection of contrast medium is necessary to visualize the target calices. Nevertheless, a combination of fluoroscopy and direct endoscopy is often necessary for a positive procedural outcome.

This kind of medical imaging carries some risks, as do other X-ray procedures. The amount of radiation that the patient and the personnel in the operative room receive varies depending on the procedure. Fluoroscopy can result in relatively elevated doses, especially for complex surgeries which require the usage of X-rays for a long period of time.

An excessive exposure to radiation can lead to injuries to the skin and underlying tissues in the short-term after the procedure (the so called “burns”), but it might also cause radiation-induced tumours in the long-term.

Fortunately, it is very unlikely that a person will encounter these complications after a fluoroscopy-guided operation. Therefore, if the procedure is considered medically necessary, the risks for the patients derived from the exposure to radiation are compensated by the potential advantages. In fact, the danger associated to the X-ray beam is usually much smaller than other treatments not related to that, such as sedation or anesthesia, or consequences from the procedure itself. To limit the exposure to X-rays, fluoroscopic imaging should be used for the shortest time necessary.

2.2.3 Patient positioning

PCA obtained under fluoroscopic guidance necessitates instillation of contrast medium to opacify the renal collecting system, which is usually done cystoscopically through rigid or flexible ureteral catheters with the patient in a dorsal lithotomy position or either prone or supine, respectively.

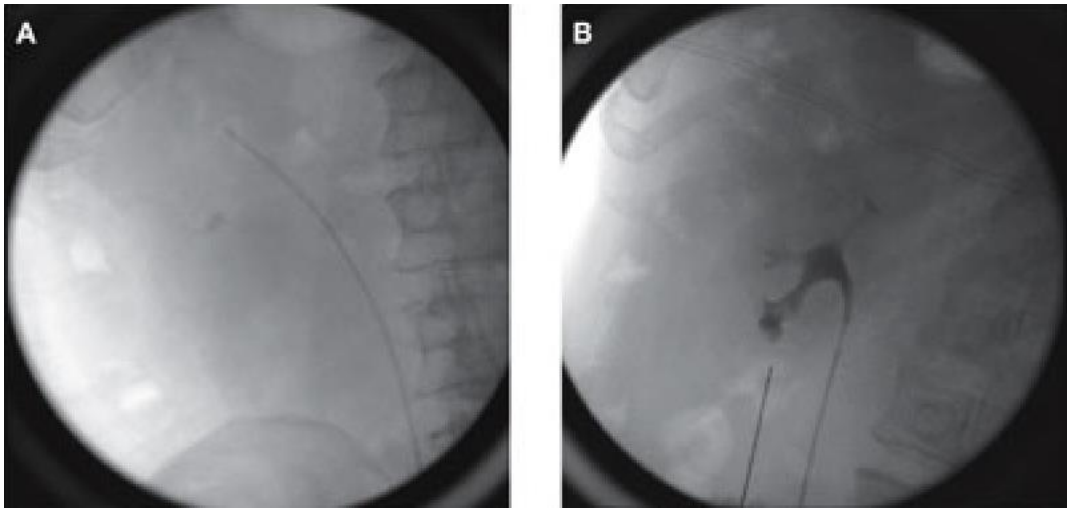

Figure 2: Fluoroscopy image A) before and B) after opacification of the renal collecting system.
[Reprinted with permission by Nature Publishing Group]

After catheter settlement the patient is positioned prone, with a foam pad under the side containing the desired kidney to be punctured, as to bring calices in a upright position and make them more easily accessible.

2.2.4 Access techniques

The standard techniques to puncture the kidney under radiographic guidance are the eye of the needle and the triangulation technique. In addition to these, a hybrid approach will be described, which integrate the standard techniques to exploit the advantages of both of them.

Eye of the needle

After catheter placement and patient positioning, the puncture needle is placed on patient's skin so that needle hub, tip and the targeted calix are perfectly in line with the C arm angled 30 degrees from the vertical position. This setup results in the classic bull's-eye effect on the radiographic screen.

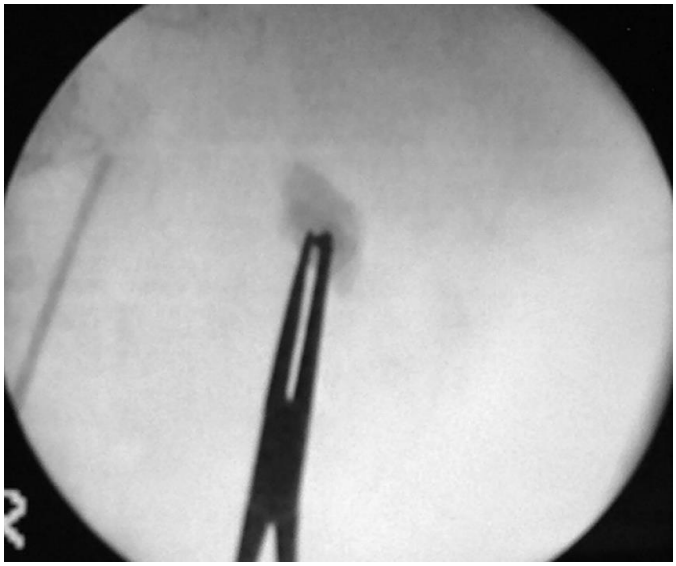

Figure 3: Bull's eye effect on the C arm monitor. [Reprinted from N. L. Miller, B. R. Matlaga, and J. E. Lingeman, "Techniques for Fluoroscopic Percutaneous Renal Access," *J. Urol.*, vol. 178, no. 1, pp. 15–23, 2007 with permission by Elsevier]

The needle is then inserted in the patient with a continuous monitoring of depth and orientation by tilting the C arm from vertical to oblique position. A correct access to the renal collecting system is then confirmed by presence of urine in the aspiration needle.

Triangulation technique

Once the surgeon has identified the ideal calix for the access, the triangulation technique is performed to determine the site of entry and orientation of the puncture needle.

The C arm is rotated from vertical to oblique position, which is usually 30 degrees. When it is in the vertical position, adjustments of the puncture line are done in the mediolateral direction, while with the tilted C arm the cephalo-caudal corrections are made.

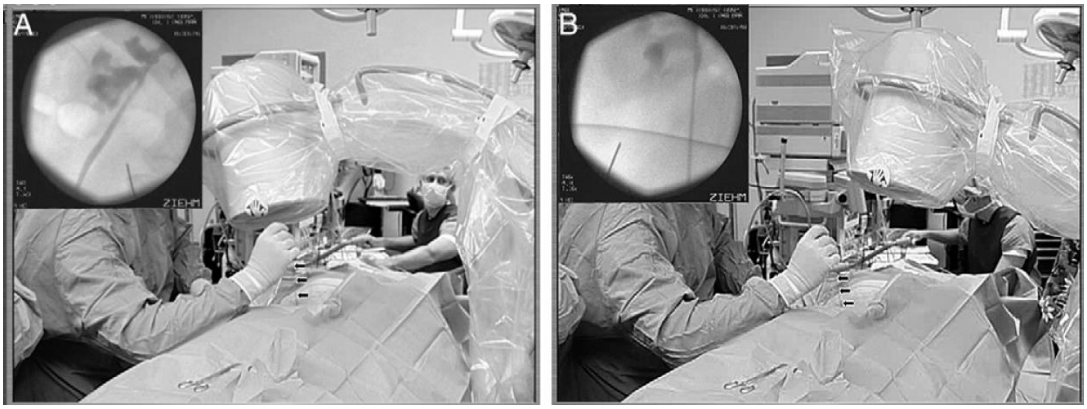

Figure 4: Triangulation technique. C arm and screen visualization in A) vertical and B) oblique position. [Reprinted from N. L. Miller, B. R. Matlaga, and J. E. Lingeman, "Techniques for Fluoroscopic Percutaneous Renal Access," *J. Urol.*, vol. 178, no. 1, pp. 15–23, 2007 with permission by Elsevier]

It is crucial to preserve the needle positioning in a plane while adjusting the other one, to maintain the correct orientation of the line of entry.
While inserting the puncture needle in the patient, continuous adjustments in the two planes are made until the renal capsule is entered.

Hybrid technique

Sharma *et al.* [5][6] have described an hybrid approach which integrates the advantages of both the previously seen techniques. After setting the subject in prone position, the collecting system is visibly delineated through a retrograde pyelography with the C arm in vertical position and the posterior calix which would allow the surgeon the optimum access is determined.

The initial puncture needle is aligned with the selected calix, producing the bull's eye effect on the C arm monitor with its overlying hub, and the correspondent site on the skin is evidenced as point A. The C arm is then rotated 30° toward the physician in the axial plane, and the initial puncture needle is held over the calix as to create the bull's eye effect on the C arm monitor. The correspondent point on the skin is marked as point B.
By aligning the needle with the infundibulum with the C arm tilted again in vertical position, the surgeon is able to determine the entry site B1 as the distance measured

between point A and B will be equal to the distance of point A and the entry point onto the line described by the needle.

The surgeon proceeds with a small incision of the skin at point B1, and inserts the needle for 1-1.5 cm. The mediolateral adjustments are made, then angling the C arm in the oblique position corrections on cephalad and caudal orientation of the line of puncture are made.

The C arm is moved back and forth to continuously adjust the line of puncture while the needle is proceeding until the desired calix is punctured, with a confirmation of a well-performed renal puncture coming from the aspiration of urine.

2.3 Medical simulators

Simulation is an essential tool for training into medical practices, as it proposes a safe, error-free environment, where trainees can fully understand and unlimitedly repeat a certain task or a whole procedure without experiencing directly on patients.

Two classes of simulation can be identified: physical simulation and computer-based simulation, also known as Virtual Reality Environments (VREs). Regarding the former, wet and dry bench laboratories can be included and then possibly subdivided into biological and non-biological models.

Cadavers and animals are used into the biological models: the former are very precise in terms of anatomy with respect to the latter, but they are definitely more expensive and of limited availability. On the other hand, animal models are much easier to find, but an ethic committee is necessary to approve and validate their use.

Physical phantoms and mannequins are incorporated into non-biological models: they are commercially and ethically accessible, but they provide the trainees with a suboptimal reproduction of the anatomy and as the biological models they are not able to offer multiple scenarios and complexity levels due to their static nature.

VR simulation overcomes many possible drawbacks of the physical simulation: it can be independent from the presence of an attendant (integrating guided tutorials) and, above all, it allows the trainees to practice on different procedures with changing degrees of difficulty. On the other hand, the efficacy of computer-based training on

traditional surgery has not been fully demonstrated; moreover, VR simulators are much more expensive than physical models.

2.4 Simulators for percutaneous renal surgery training

Percutaneous renal access (PCA) is considered one of the most arduous step in percutaneous surgery for kidneys: the proximity of the kidneys with vital structures like the liver, the spleen, the colon and the lungs leads to the need for a strong preparation of the surgery, and the identification of the correct approach to decrease the risk of haemorrhagic complications and damages to the surrounding organs.

Watterson *et al.* [7] report that while percutaneous surgery is performed by urologists, barely one in ten obtains renal access himself, and in the other cases PCA is obtained by interventional radiologists: the causes include the reduction of time inside the operating room, personal preference and a better equipment accessible from radiologists, but the main reason is the lack of training during urology residency.

The struggle in achieving competency by taking part to real percutaneous renal surgery stresses the need for medical simulators, useful for obtaining confidence with unlimited repetitions of this procedure in an environment free from radiation exposure. Noureldin *et al.* [8] have reviewed the state of the art for PCA simulators and identified several models for the training, including live animals, biological and non-biological bench, cadavers and virtual reality-based environments.

2.4.1 Biological bench simulators

Ex vivo animal structures were used for percutaneous renal puncture simulation: as for size and shape, porcine and bovine kidneys are the closer to the human ones. For this reason, the majority of the studies about PCA with biological models integrate them with a wrapper to hide the internal structures and with some other parts of the body, like the ureters. The kidneys are usually stabilized into foams or gels and placed into chicken carcasses [9], skin flaps [10][11] or into physical human-like mannequins [12], in order to be visible through the fluoroscopic or ultrasound guidance during the training.

A biological bench model with a live anesthetized pig was used by Kallidonis *et al.* [13] to assess the feasibility of training in PCA, and it is the only one reference to live animals for percutaneous renal surgery simulation in literature.

Biological bench simulators are usually low-cost models with the advantage of a haptic feedback comparable to human body, but they lack in correctly reproducing the anatomy, they are subject to wear and tear, and there are ethical considerations to be considered with biological models.

2.4.2 Non-biological bench simulators

To overcome the limitations of anatomy distortions seen in the biological models, non-biological bench simulators include rapid prototype replicas of human structures surrounded by foam or wrapped into mannequins.

In the study of Bruyère *et al.* [14] a virtual kidney was created from the CT of a patient undergoing kidney stones removal surgery, with a balloon connected to a respiratory machine as to emulate the displacement of the kidneys in the respiratory phases. Zhang *et al.* [15] developed a non-biologic set-up including a kidney, ureteral stamp and the possibility to choose among several models with calices oriented in different directions. Silicone models were used also in the investigation of Turney *et al.* [16], in which the collecting system was extracted and segmented by CT urograms and then 3D-printed to obtain an accurate reproduction of human kidney anatomy. These bio-models were then filled with contrast medium and placed into a thick layer of foam to emulate the tissue between kidney and skin.

Non-biological simulators are able to perfectly replicate human anatomy, to provide optimal tactile feedbacks and with the correct choice of the materials even to allow the common imaging techniques used in real surgery. However, preparation of these bench models implies a considerable amount of time and money, and as the biological simulators, they get consumed over time and by usage.

2.4.3 Virtual reality simulators

Regarding percutaneous renal surgery, only the PERC Mentor™ (Simbionix) [17] has been validated as a tool for training into PCA [18][19][20][21]. This VR simulator is designed into procedural steps to realistically perform the PCA and verify

the correct access to the kidney, and it is able to provide a quantitative and a qualitative evaluation of the performance. The PERC Mentor™ platform allows the user to choose among several normal weight or obese virtual patients, with different renal anatomies and pathologies, and to manipulate 2D fluoroscopic radiographic images through a simulated C arm to obtain renal access with needles of various length and size inserted in a torso mannequin.

Figure 5: The PERC Mentor™ [Simbionix][17]

While biological and non-biological models are subject to degradation, procedures simulated in a virtual reality environment can be indefinitely repeated, with scenarios of changing difficulty. Furthermore, simulation of fluoroscopic guidance protects the trainees from unwanted radiation exposure, and the simulators could provide an evaluation report at the completion of the task.

The main reason of the underutilization of virtual reality simulators is the cost: as reported in [8], the PERC Mentor™ is on average twenty times more expensive than models created with rapid prototyping and a thousand times more expensive than biological bench models, preventing an extensive exploitation in the medical training field.

2.5 Haptics in medical training

One of the most important physical senses in medical procedures is the sensation of touch, either by directly manipulating tissues or by handling a surgical instrument. For this reason, haptic devices applied to medical simulators have become a valid alternative for training, as they are able to convey the sense of touch to the trainee in a virtual reality environment. The integration of these devices has led to an increase of the realism in the simulation of procedures, and consequently has enhanced the quality of the training compared to standard learning environments of medical schools.

Haptic devices are electro-mechanical apparatuses able to add tactile feedbacks to a virtual environment, with different degrees of freedom depending on the movements in the space they can allow the user to do; current haptics-based simulators include haptic devices with three or six degrees of freedom. At the moment, there are two modes of controlling interaction of the haptic devices with the virtual scene: admittance or impedance control.

Regarding the admittance control, the force applied to the haptic device is translated in a relative distance, which is used to provide the user with the proportional force feedback.
Their complexity is translated into an enlargement of the device itself, which prevent them to be widely spread in the medical simulation field.

In the impedance control, the movements of the device are coded and transmitted to the computer, and the application itself is responsible for generating and monitoring the feedbacks. The apparatuses which use the impedance control are therefore smaller and easy to connect and integrate to a work station. The most widely commercialized haptic devices with impedance control are Phantom® (Geomagic®) [22] and Falcon® (Novint Technologies Inc®).

There are numerous types of medical practices simulated with haptics-based applications with the aim of training:

- **stitching procedures** usually require a haptic device with six degrees of freedom, to simulate the torsion of the surgeon's hand while piercing the dermis layer;
- **palpation** consists in the digital analysis of tissue or organs by the physician, to

detect irregularities on their surface. Palpation is effective for distinguishing different areas by their stiffness, as sometimes stiffer regions might be correlated to tumoral masses;

- common **dental procedures** like calculus and caries removal are extensively simulated with haptics-based environments replicating the real workstations;
- **endoscopy and laparoscopic procedures** are minimally invasive surgeries and they are performed with two hands: therefore, their simulation requires the use of two haptic devices, and provides the trainee with practice in endoscopy navigation and in video laparoscopic surgery;
- **orthopaedics** is mainly related on interaction with bones, and therefore the focus for the simulation of this surgery is on drilling and on realistic force feedbacks;
- **biopsies** consist in the sampling of human tissue with a needle for the analysis of cells and detection of pathologies, like cancerous regions or inflammation in the organs.

Several biomedical companies has developed haptics-based workstation: CAE Healthcare, Inc. [23] commercialized CAE NeuroVR™ for the training in neurosurgical procedures and CAE LapVR for laparoscopy simulation. Both of these workstations provide the trainees with different modules of changing degree of difficulty, and an enhanced realism due to the combination of haptic devices for tactile feedback and real surgical instruments. Surgical Science, Inc. [24] released LapSim®, an integrated simulator used for training into several laparoscopic procedures. The trainees can practice into suturing, clipping and grasping organs and tissue, with a real-time tactile feedback and visualization of the laparoscopy monitor. Immersive Touch, Inc. [25] produced a simulator with augmented and virtual reality technology for surgical planning and training in minimally invasive surgery. Each one of the simulators that have been mentioned can also provide performance feedback and evaluation of the trainees, adding a quantitative assessment of their capabilities and improvements time after time.

Figure 6: Left: LapSim® [Surgical Science][24]. Right: CAE NeuroVR™ [CAE Healthcare][23].

Chapter 3

3. Approach[2]

3.1 Motivation

Nephrolithiasis is an extremely common pathology in the United States, with an occurrence of 7% in women and 13% in men, approximately. Consequently, the economic burden from kidney stones is significant, with an assessed $4.5 billion related to healthcare expenses, and this amount is predicted to increase with time [26].

Percutaneous nephrolithotomy (PCNL) is the standard of care for large renal stones removal (> 2 cm in diameter), and it is expanding as a valid alternative for the treatment of complex and lower-pole stones of medium and small size [12].

In the United States, this treatment method registered a growth in the rate per year from 17 to 31 per million adults in the period from 1998 to 2011 [26]. Its increase is due to several factors, including the overall rise in prevalence of kidney stones disease, but especially to the improved stone-free rates offered by PCNL compared to the more minimally invasive approaches when handling large or complex calculi.

This procedure is associated with the risk of adverse, or even fatal outcomes; the development of fine surgical skills as well as extensive training is crucial for reducing the incidence of major complications: it has been shown that at least 24 PCNL procedures are needed for a surgeon to achieve a good proficiency, while competency and expertise arise after 60 and >100 cases respectively [27].

Establishing percutaneous renal access is the most challenging step of this surgery, and the steep learning curve involved for physician to gain experience in the procedure in mainly attributed to the preliminary renal puncture. While an appropriate

[2] *This chapter has been mainly taken from the work of the author at* [38].

training is necessary, in the traditional method of learning in medical schools surgeons accumulate experience only by participating in the operative room. The restriction of the working hours in many countries has challenged the standard model of medical training, and could lead to a potential decrease of surgical quality [28]. The purpose of the policy for reducing working hours was to concede time for the physicians to rest and keep a good psychophysical status, achieving improvements in the outcomes for and the care of their patients.

However, in surgical training expertise is obtained by practising the procedures repetitively under control by trainers during the learning phase. Step by step, by gradually increasing the "hands-on" experience, the trainee would finally perform the whole procedure proficiently. Without an appropriate exposure to real surgeries during their training period, trainees might not get enough skills to master more complex procedures, including PCNL. Consequently, after their residency programme they could still be in their learning phase, and thus be performing operations with no adequate supervision. Eventually, the health of patients might unexpectedly be endangered because of the same policy that aimed at its improvement.

A study by Watterson *et al.* [7] confirms the inadequacy of the training in percutaneous renal access: only 11% of the urologists performing PCNL habitually acquire percutaneous access themselves. Explanations for this trend may include insufficient capabilities and the persistent opinion that PCA is a radiological procedure and that is therefore the interventional radiologist who should be responsible for it. On the other hand, in a research of 103 patients aiming at the comparison of the outcomes in the case of interventional radiologist-gained access versus urologist-gained access, further support for urologists training in PCA was outlined, as lower clearance of the kidneys (61% versus 86% respectively) and more complications (28% versus 8% respectively) were found when the procedure was performed by interventional radiologists [29].

Because of the working-hour reduction and increased awareness of the potential risks to patients during the training of surgeons, it is necessary to abbreviate the learning curve for surgical operations. Several training models had been introduced to ease the acquisition of skills for renal puncture before trainees undertake the procedure in patients, and each of them has advantages and disadvantages.

Bench models made of synthetic materials provide easily accessible, repeatedly useable approach. However, the poor tactile feedback is the main drawback of these models, that are also easily degradable and sometimes quite expensive.

Besides the “dry laboratory” training there are also training models that include the use of parts of animals (“wet” laboratory training). Literature reports the use of porcine and bovine kidneys for training, either as truncated parts or embedded in silicon. The use of live animals for training in PCA is also practicable. The main advantages of these animal mock-ups are that they are low-priced and the provision of tactile feedbacks during the task. Apart from the bioethical concerns, biological bench models present some drawbacks. These comprise: (1) The arrangement is costly and labour demanding; (2) The anatomy and material characteristics of animal tissues are altered from human structures; (3) The organs show large dissimilarities and rapidly start to worsen.

While biological and non-biological models are subject to degradation, tasks in virtual reality simulators can be indeterminately repeated, with settings of increasing difficulty. Furthermore, emulation of radiographic guidance protects the trainees from radiation exposure, and at the end of the training session the user can obtain quantitative results and feedbacks regarding his/her performance. There are some limited disadvantages of percutaneous VR simulators which are worth considering. They are costly to purchase, may have high maintenance costs and haptics can be unreliable.

In all the surgeries, and as well in percutaneous access to the kidneys, sense of touch is along with sight the most important feedback to the physician, therefore an effective simulation of the procedure for training purposes should convey to the trainees an integrated and comprehensive understanding of all the stimuli that they will experience in the operating room.

Haptic devices applied to medical simulators have become a valid alternative to standard learning methods in medical schools: haptic emulated surgery is a novel training option, serving as a real case simulation platform for education, and preoperative preparation for difficult anatomical situations.

After literature review and analysis of the state of the art, we identified the need for an easily accessible, anatomically precise training model for the urologists desiring to improve skills development in gaining percutaneous renal access: the actual

procedure is technically complex and presents a steep learning curve, and the current training models are either inaccurate, highly priced or subject to quick degradation. They might also involve the exposure to radiation, and in the case of virtual reality simulators, they are not provided with haptic feedback, that along with a correct reproduction of the human anatomy, is a critical element in all the medical simulation models.

3.2 Proposed solution

With the goal of meeting all the disadvantages that were found in current training models, an optimal solution should allow for skills improvement in a risk-free environment, reducing unnecessary radiation exposure for patients and personnel in the operative room as trainees get experience in real-time screening during the task. The training should aim at the acquisition of hand-eye coordination, C arm manipulation and the development of skills in processing 2D fluoroscopic images into 3D mind images. This tool should be economically accessible for medical schools and convey the visual and the tactile stimuli of a real operation to the trainees, enhancing the realism and accuracy of the training environment and shortening the learning curve of the procedure.

By addressing these specific requirements, the proposed solution is an augmented and virtual reality scene composed by 3D anatomical phantoms and an emulated fluoroscopy guidance. A virtual environment is easily modifiable, and it is not affected by degradation, delivering a durable device. The fidelity of the human anatomy could be preserved as the models of skin, spine, kidneys, ureters, lungs and vessels are extracted from a real patient's volumetric dataset; the volume itself could be explored, offering a radiation-free navigation system able to perfectly mimic the C arm unit used to obtain a real-time radiographic image of the patient.

Kidney puncture could be accurately simulated by haptic technology, providing the clinician with accurate anatomical orientation and a step-by-step tactile feedback ideal for the acquirement of puncture skills.

Aiming at the cost containment of the overall simulator, in the development of the platform a bunch of pre-existing software could be comprised, to obtain good

performances in term of haptics and graphics rendering. The application could run on a common computer, so that the only additional component needed could be a haptic device, which is now buyable at reasonable price.

Chapter 4

4. Implementation[3]

The aim of this research is to develop and evaluate an anatomically accurate, low-cost haptics-based virtual reality surgical simulator for percutaneous renal access. To correctly mimic the procedure, the virtual environment will include the 3D models of the structures of interest which the user will interact with, and the volumetric dataset where these meshes will be extracted from, to emulate the fluoroscopy guidance.

The operative room provides the surgeon with visual and haptic feedbacks, and so will do the simulator: the 3D models will have tactile properties that the trainee will feel throughout a haptic device, and a stereoscopic view of the scene will be implemented to convey to the user a proper perception of depth.

Taking into consideration these requirements, the steps to implement the application will include an initial phase of segmentation of the image and extraction of 3D models of the kidneys and the collecting system, the skin, the spine and the ribs, vessels and lungs. These meshes will then need to be processed to make them computationally lighter as to comply to the specifications of the virtual environment, that is requested to comprise both a visual and a haptic representation of the models. The need for a powerful and efficient augmented-reality scene has led to the development of a platform able to integrate and exploit specific libraries for graphics and haptics rendering. This chapter will then cover the preliminary phase of segmentation of the image, the refinement of the extracted 3D models, the software development and the implementation details of the simulator.

---

[3] *This chapter has been mainly taken from the work of the author at* [38].

4.1 Image segmentation

The process of subdividing an image in homogeneous regions, where all of the voxels related to a certain anatomical structure are grouped together, is called image segmentation.

The grouping of the pixels is based on a homogeneity criterion that distinguishes an area from the others. Image segmentation could be performed manually or automatically. The former is more accurate, but it is extremely time-consuming, as the user is responsible for contouring the region of interest (ROI) in each slice of the medical image. The latter instead allows the user to obtain an extremely faster segmentation, but it is not as precise as the manual one in defining extraction contours, and consequently it might lead to the extraction of unwanted areas.

In this work, automatic segmentation based on the Thresholding method was used to grossly define the different anatomical regions, and manual segmentation was then performed to improve the extraction contours.

Thresholding is a region-based segmentation method in which the image is divided in different areas according to the similarity of the gray levels associated to voxels. In the case of anatomical images, the choice of using this type of automatic segmentation is legitimized by the fact that each region has usually a gray level which is different from those surrounding, as points belongings to the same structure (Kidney, for example) possess the same degree of absorption of the radiation. Before the actual segmentation process, the image is pre-processed, to avoid the artefacts introduced by low contrast and noise which are generally present in medical images. Consequently, contrast will be adjusted to highlight the region of interest, and the noise will be reduced by increased smoothing, which allows to filter the signal and make the image clearer. The need to make these preparations and then proceed to an automatic image segmentation has directed the project towards the use of software for image segmentation, and the choice fell on itk-SNAP™.

itk-SNAP™ [30][31] is an open-source software used for segmentation of 3D medical images. The dataset is loaded on the home screen, in its sagittal, frontal and transverse projections. The anatomy is visible layer by layer by moving the cursor to scroll the slices. Through the graphical interface the user is able to change the image

contrast highlighting the areas of interest. The software allows the user to perform the automatic image segmentation according to the Thresholding method: the threshold value is set by manipulating the spectrum of the gray levels, and adjusting the smoothing it is possible to better define the parts of the image that will be segmented (in white) from the ones that will be discarded (in blue). The area that will be segmented expands from seeds positioned by the user.
When the result is satisfactory, the expansion is interrupted and the volume rendering image of the extracted image.

The volume used to segment the models was taken from the DICOM Image Library by OsiriX© [32]: the choice fell on the dataset CALIX, as it comprises several DICOM datasets from the same patient highlighting different anatomical structures, and in particular the renal collecting system.

itk-SNAP™ finally allows the exportation of the segmented image as a mesh in .STL format: a .STL file ("StereoLitography") allows to describe and represent a three-dimensional surface through its discretization with a series of triangles. Essentially, the .STL file consists of a list of data that uniquely identifies the triangular faces covering the surface by means of the spatial coordinates of its vertices and of the normal to the triangle. Consequently, each triangle that forms the mesh will add to the .STL file twelve coordinates. Each triangle of the mesh must necessarily be connected to the next by sharing two of its vertices, and all the coordinates that constitute the file must be positive. The .STL format is used primarily in the rapid 3D printing and prototyping. The exportation of a mesh is crucial: the 3D models need to be elaborated and processed before adding them to the virtual environment, as it will be explained in the next chapter.

4.2 Post-processing of the 3D models

One of their biggest issues of meshes extracted from medical images is the high surface roughness: in the human body, many organs and tissues show a similar absorbance of X-rays, so that in the CT images elements close to each other can be represented by similar levels of gray, making it difficult to identify a specific structure with respect to another. Contrast media are usually used to alter the absorption of X-

rays of a tissue or organ, making it more visible or less. In the CT image used for this work a medium has been introduced into the ureters to highlight them. This substance is not evenly distributed throughout the volume of the ureters, so what is extracted is not the actual size of the structures of interest, but their volume traversed by the agent of contrast, thus creating in their virtual reconstruction very rough substrates, that need to be smoothed.

The meshes obtained from segmentation need also to be carefully decimated; not only to preserve the anatomical topology of the surface, but to maintain an adequate number of polygons for the haptics libraries to perform adequately at the framerate described above.

To achieve these two main goals, smoothing and decimation, ParaView™ [33] and 3ds Max® [34] were used. ParaView is an open-source, multi-platform data analysis and visualization application, which supports a wide variety of visualizations algorithms including advanced techniques such as contouring, polygon reduction and mesh smoothing. 3ds Max® is an open-source (in its student edition) 3D software for modelling, animation, and rendering.

4.3 Software development

The requirements for this work include the integration of a highly-defined graphics rendering and haptics rendering through a haptic device. The haptic device used for this project is a Touch™ 3D Stylus (3D Systems Geomagic®) [35]. Its technical specifications are summarized in Figure 7.

(a)

Type	Touch 3D Stylus
Positional Feedback	6 (complete pose)
Force Feedback	Dof 3 (position only)
Force Feedback workspace (WxHxD)	10.45 x 9.5 x 3.5”
Maximum Force	3.4 N
Nominal position resolution	0.084 mm

(b)

Figure 7: a) Touch 3D Stylus and b) its technical specifications.

The user interface of the haptic device is handled by QuickHaptics™ Micro API [36], a library that allows the user to create basic haptics-based applications. The built-in graphics rendering of QuickHaptics™ is however limited in the performance and in the representation of objects in the scene, as the only displayable items are either meshes or geometric primitives. As the volumetric rendering of CT images simulating fluoroscopy are crucial in this work, the necessity for an alternative tool for representing 3D images emerged.

To supply for the limitations introduced by QuickHaptics™, an external graphic library was needed to be integrated in a unique platform able to give the user good performances in terms of haptics and graphics rendering, and it was decided to choose Visualization Library [37]. Platform development resulted in the creation of a library based on C++ coding language called *LACE Library*, whose features and details of implementation will be explained in the following chapter.

4.3.1 Design of LACE library

The development of an integrated platform occurred from the need for virtual reality-based applications with a robust graphic interface and haptics rendering. The implementation of *LACE Library* is the result of a joint work with three colleagues from the bioengineering department at the University of Illinois at Chicago, as the requirements and the field of application of this tool were comparable [38][39][40][41].

LACE Library integrates and manages the interactions between four different software-hardware environments:

- Visualization Library (VL) is an OpenGL based open-source library for 2D and 3D graphics application. The library maintains the flexibility and high performances of OpenGL API, with intuitive and user-friendly classes and functions, and it is responsible for the graphics rendering of the virtual scene;
- QuickHaptics™ (QH) is a haptic library developed in C++ and built on top of Geomagic® OpenHaptics®, the software development toolkit implemented for 3D System haptic devices. QH is used to manage the force feedback;
- Wykobi Library (WK) [42] is a C++ 2D-3D computational geometry library for fast mathematical calculation;
- Ascension 3D Guidance (AS) [43] is a 3D electro-magnetic tracking system, which allows the easy communication with a tracking unit through 3D Guidance API.

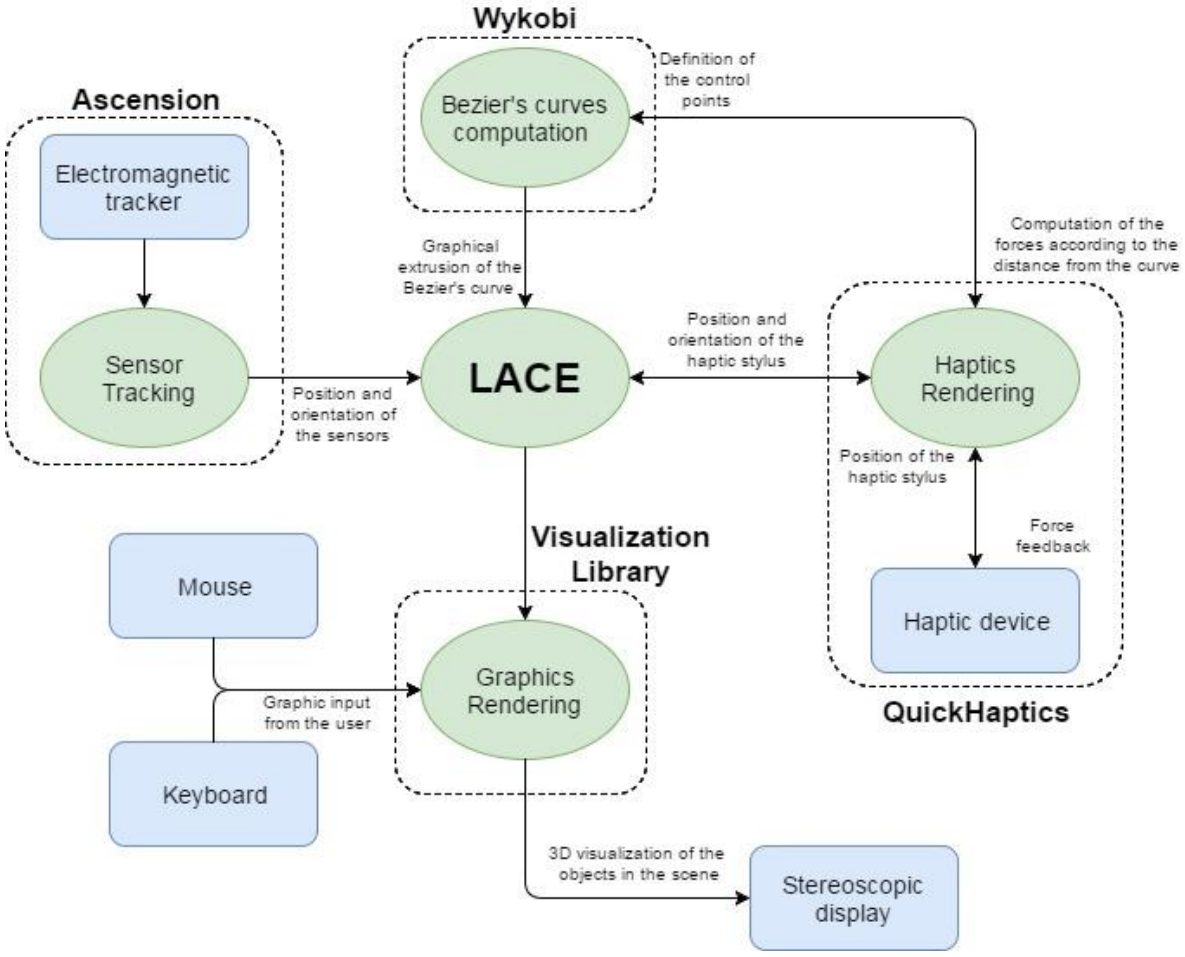

Figure 8: General implementation and logic of *LACE Library*.

The aim of *LACE Library* is to give the user the possibility to create applications based on the interaction between these four libraries. The general logic behind communications and functioning of *LACE Library* is showed in Figure 8.

LACE Library has been organized as two different threads on a Windows platform that run concurrently: the graphics visualization is rendered at 60 Hz (30 Hz for the left and the right views when the stereo modality is active), while the haptic servo loop cycles at 1000 Hz.

In *LACE library* VL functionalities are exploited to manage all the processes related to graphics display. The visual features of the objects in the scene can be regulated by the programmer and by using the mouse and the keyboard the user is able to interact with the scene through custom-made call-back functions.

QH is responsible for haptics rendering. The programmer can either take advantage of the pre-made functionalities of this haptic library or implement his/her own algorithms.

The communication between VL and QH is managed by *LACE Library* so that all the objects in the scene and the haptic device are correctly mapped and displayed in the graphic environment.

WK allows the user to achieve efficient mathematical calculations and improve the computational performances needed for specific applications. With AS, the programmer is able to insert tracking items based on electromagnetic sensors in his/her implementations. Ultimately, an integrated platform such as *LACE Library* provides the developer with a user-friendly and efficient tool for implementing applications in an augmented reality environment.

LACE Library is composed by several classes. To better describe the function of those classes, they can be divided in four groups:

- Renderable Objects: it includes the classes used for the creation of the objects that can be visually and haptically perceived in the virtual scene. The classes belonging to this group inherit from the base class LACE_Object, that handles the communication between QH and VL. With *LACE Library* it is possible to create objects like volumes, meshes, extrusions and images, in addition to the basic geometric primitives;
- Tracking System: this group comprises the classes LACE_Transmitter and LACE_Sensor that are responsible for the communication with AS;
- Special Force: LACE_VolumeForce and LACE_ForceField are the two classes belonging to this group. Those classes can be associated respectively to a LACE_Volume and a LACE_Extrusion in order to define special force fields to be rendered;
- Rendering classes: *LACE library* allows the creation of multiple renderings in the scene; each rendering is defined as a LACE_Rendering class instance. This class contains both a list of the objects to be rendered and all the rendering parameters of the camera and the viewport. In this group it can be included also the class LACE_CuttingPlane, that gives the user the possibility to cut one or more LACE_Object instance.

Pointers to all the classes used by the programmer in his/her specific application are stored in LACE_Class, a singleton class that must be defined in each program based on *LACE Library*. This is the most important class, as it handles the initialization and update processes, and contains a lot of functions available for the users to customize their executables.

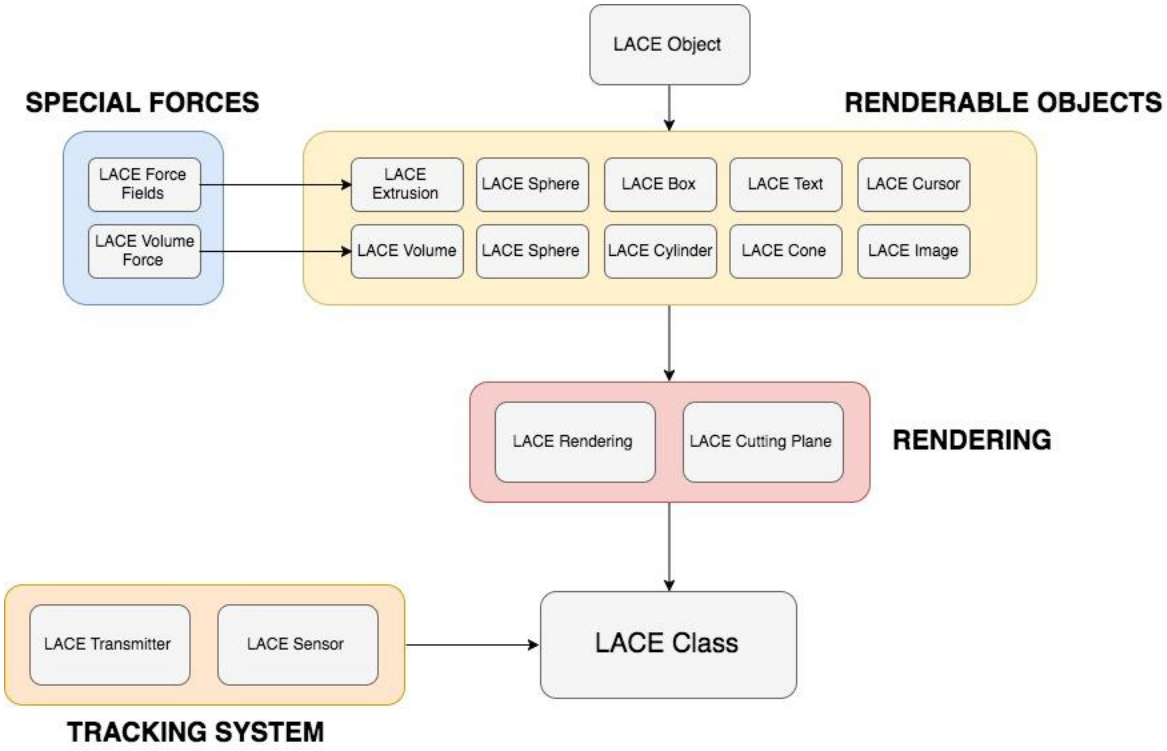

Figure 9: Classes in *LACE Library*.

All the objects that can be graphically created in *LACE Library* inherit from a base class called LACE_Object. Each LACE_Object has an associated actor (VL_Actor) which is linked to a geometry (VL_Geometry), a transform (VL_Transform) and an effect (VL_Effect). LACE_Object also contains the pointer to the corresponding QH shape (QH_Geometry), so that the haptic properties of the specific shape could be directly modified using QH functions. The presence of a base class common to all the objects, containing shape-specific variables and parameters, was needed to properly render the scene and its components and to allow the communication between VL and QH. A scheme of the class LACE Object and its organization and interaction with QH and VL is reported in Figure 10.

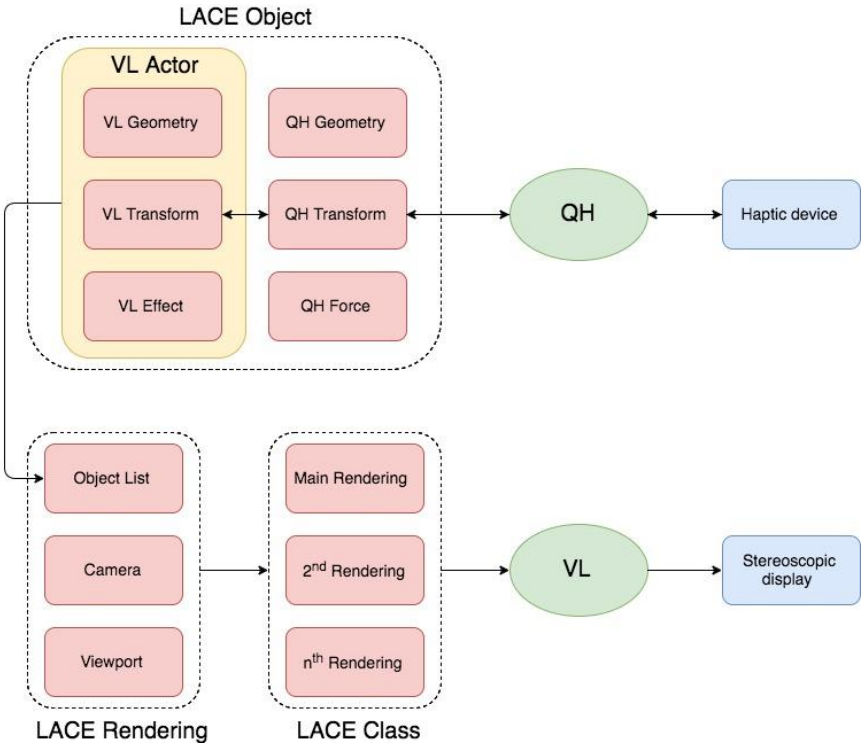

Figure 10: LACE Object class and its communications

After their creation, the objects are added to the main rendering to be displayed into the scene. LACE_Object comprises the two variables that allow to manage the exchange of information between VL and QH: VL_Transform and QH_Transform. They represent the transformation matrices that define the rotation, translation and scaling of each object in VL and in QH. To make the two environments consistent they always need to be equal.

Two cases can be considered in which the transform of a shape is changed:

- when an object is added to the scene, the transform takes into account an object-dependent transformation given by default for some specific objects for rendering purposes, and an eventual user-defined initial transformation. At this stage, the communication process modifies VL_Transform first and then sets QH_Transform accordingly, if QuickHaptics™ is being used.
- while the application is running, with an update of the transform: this second scenario is the one that always applies to the graphic cursor, which can be either the haptic device or the electromagnetic tracker, or both. At each graphic frame,

the QH_Transform or the AS_Transform are automatically updated by either QH or AS, respectively, and then VL_Transform is updated accordingly.

The logic behind the management of the transformation of the objects and the communications between the libraries is shown in Figure 11.

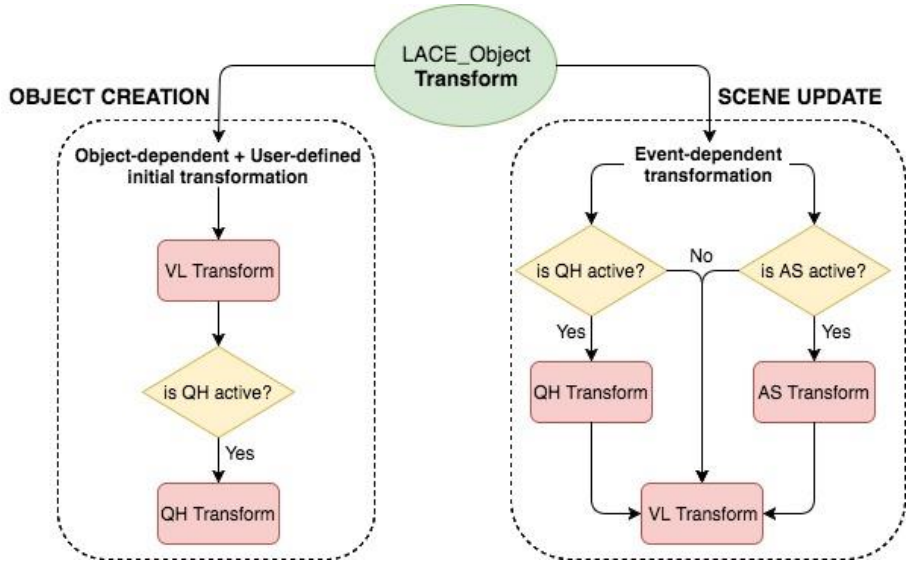

Figure 11: Management of transformations of the object in *LACE Library*.

4.3.2 Implementation details

Figure 12 shows the logic behind the implementation and the processes occurring in the application. The scene is composed by the 3D models of kidneys, ureters, skin, spine, spleen, lungs and vessels, with their own haptic and graphic properties. The user is able to modify these features through a graphical user interface (GUI) implemented with GLUI, a GLUT-based C++ library.

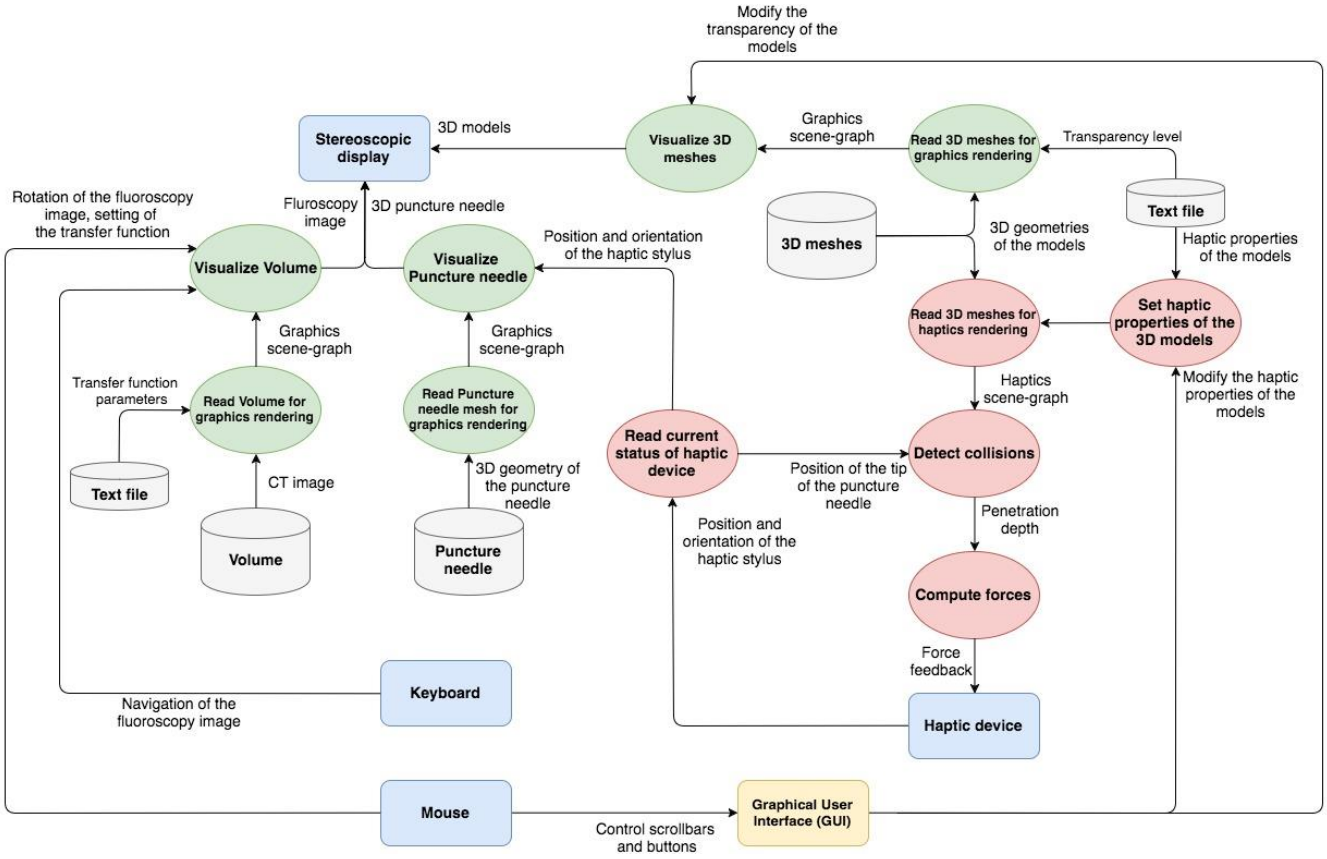

Figure 12: Scheme of the implementation details

The different shapes in Figure 12 distinguish the processes (circles) that occur in the simulation from the hardware components (squares) and the data (cylinders) used in the simulation.

Hardware components

a. Haptic device, as presented in Figure 7, to convey the sense of touch of the virtual environment to the user;
b. Stereoscopic display, to provide the user with depth perception, implemented with the off-axis projection method, as explained in the following chapter;
c. Mouse and keyboard, to interact with the GUI (Chapter 4.3.5) and control the fluoroscopy image.

Data

a. CT image: as described in Chapter 4.2, the volumetric image used to extract the virtual models was taken from the open-source repository DICOM Image Library by OsiriX© [32];
b. Virtual models: segmented and extracted from the CT image, as described in Chapter 4.2;
c. Virtual needle: created with 3ds Max® [34] and imported in the scene as a .OBJ;
d. Text files: they contain the initial values of the haptic and graphic features of the virtual models (transparency, stiffness, damping, friction and pop-through) and the parameters of the transfer function for the visualization of the volumetric image.

Processes

The different colours in Figure 12 are referred to the two main processes that handle the simulation:

- **Graphics rendering** (green): it comprises those steps related to the visual aspects of the simulation. It handles the reading of the data for the visualization of the virtual models and the fluoroscopy image. The graphic thread is totally supported by Visualization Library;
- **Haptics rendering** (red): handled by QuickHaptics, it includes the reading from text file of the values of the haptic properties to be rendered, and most importantly, it is responsible for the tracing of the haptic device in the space, which is essential in the detection of the collision and in the computation of the forces, as explained in Chapter 4.3.4.

A graphical representation of the workflow of the simulator, with particular attention to the interaction between hardware components and the patient's data, is presented in Figure 13.

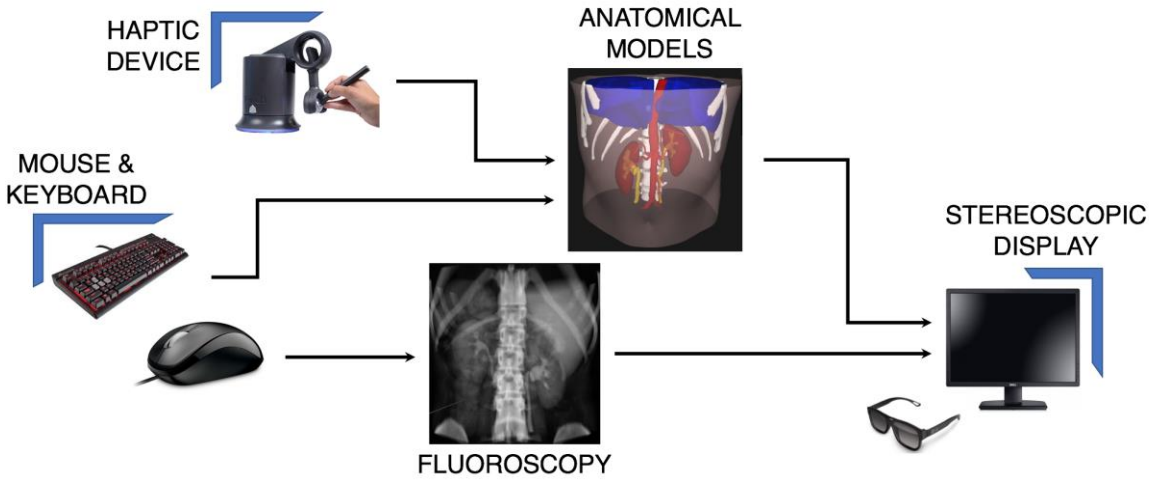

Figure 13: Application workflow

4.3.3 Graphics rendering

The 3D models extracted from the volumetric image are added to the scene as LACE_Mesh instances: with the LACE_Mesh class the user is able to load 3D shapes in the formats supported by VL (.3DS, .STL and .OBJ, to name a few).

A polygonal mesh in *LACE Library* can be associated to the volume from which it has been segmented, obtaining the default match of these objects, or directly added to the scene with its own specific offset. As a LACE_Object, textures or colors can be assigned to the LACE_Mesh, and it is subject to the all the functions defined in *LACE Library*.

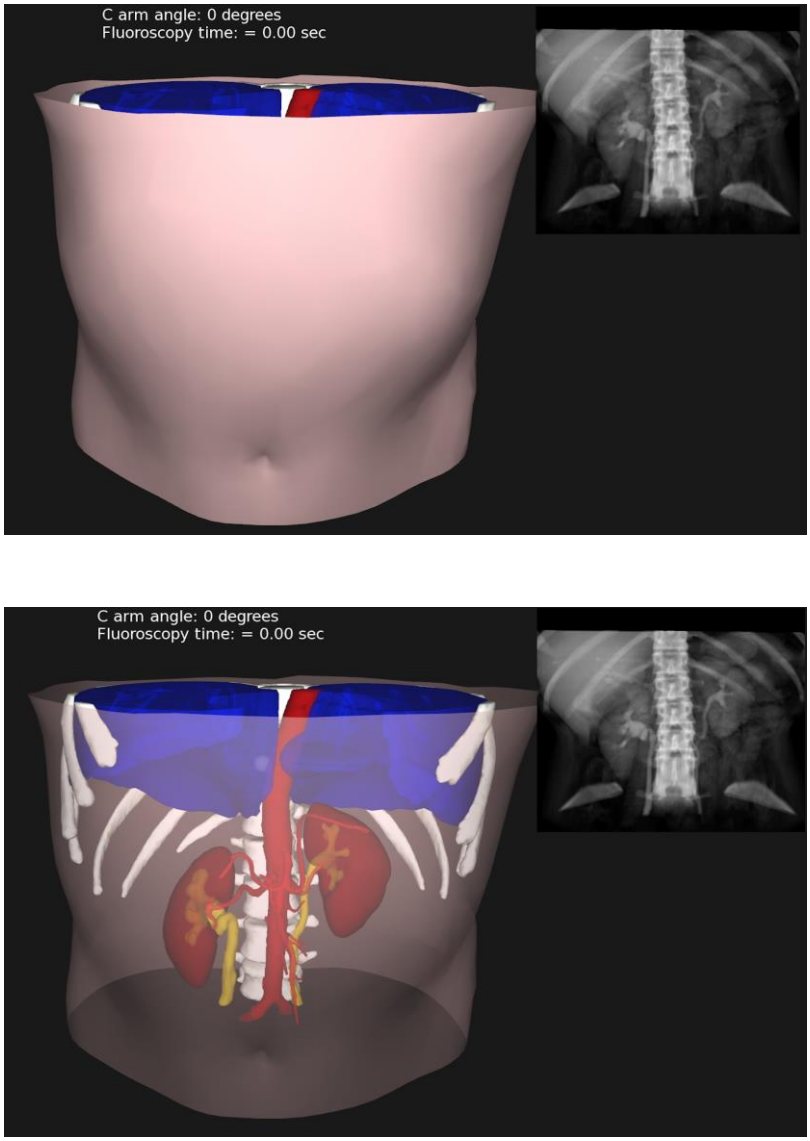

Figure 14: Visual interface of the simulator with Up) opaque and Down) transparent models.

Modern medical image equipment such as CT and MRI produce vast amounts of data in the form of arrays of slices. Although they are a complete volumetric representation of the scanned patient anatomy, these datasets can only be observed as a set of 2D images, when observed by a radiologist. Therefore, volumetric rendering not only provides a method to graphically display the 2D medical information to a more intuitive 3D representation, but it also offers a method to obtain accurate and detailed anatomical 3D models for haptic rendering and simulation.

The volumetric dataset is loaded in the application as a LACE_Volume instance. LACE_Volume is the class in *LACE Library* that manages the creation and setup of the

volumetric images. This class allows the user to load and display DICOM images and MHD files, which are the most common format for storing medical volumes such CTs and MRIs.

Three ways of volume visualization were implemented:

- volumeSLICED is made up from slicing the volumetric data and then reassemble the cuts into an image. The user can choose the number of slices and define the visible parts of the rendered volume by setting an Alpha Test value with which the values of the voxels are compared to;
- volumeRAYCAST takes advantage of the Raycasting technique to render a volume. The programmer can decide between multiple predefined raycasting methods, such as Maximum Intensity Projection or Brightness Control, and set the level of opacity of the rendered image;
- volumeORTHOGONAL consists in the reconstruction of the three orthogonal planes that are commonly visible in software and applications for the exploration of medical images; sagittal, coronal and axial planes can be displayed based on the position of the haptic device or the sensor, or by fixing the coordinates of the intersection point of the three views.

For these visualization modes a custom-made transfer function for the R, G, B, and A channels can be tuned and controlled, and as a LACE_Object, all the functions defined in LACE can be applied and updated by the user. In the application, the volume is rendered in the volumeRAYCAST visualization mode on a framebuffer object to optimize and lighten the graphics rendering.

In *LACE Library*, the user is allowed to define as many scenes as he/she desires, and choose whether to render them on a texture attached to geometries in the main rendering or to a sub-rendering by dividing the screen in multiple viewports.

The trainee can practice on the desired access technique under a real-time fluoroscopy guidance. As in real surgeries, the emulated C arm can be moved all around the models, showing the correspondent fluoroscopy image on the screen: rotations, translations and zooming are enabled to give the trainee a reliable and realistic navigation system, by which keeping track of the position, depth and orientation of the puncture needle inside the body structures.

The fluoroscopy is rendered as a volume with the ray-casting technique. In its basic form, the volume ray casting algorithm comprises four steps:

1. **Ray casting.** For each pixel of the final image, a ray of sight is cast through the volume. It is useful to consider the volume being enclosed within a bounding primitive that is used to interconnect the ray of sight and the volume.

2. **Sampling.** Along the part of the ray of sight that lies within the volume, equidistant *sampling points* are selected. It is usually necessary to interpolate the values of the samples from its surrounding voxels (commonly using trilinear interpolation).

3. **Shading.** There are two values associates with each sampling point: **c(X)** - a shade calculated from a reflection model using the local gradient and **α(X)** - an opacity derived from tissue type of known CT values. Samples are then *shaded* (i.e. coloured and lit) according to their surface orientation and the location of the light source in the scene. The value associated to each voxel is derived from the composition of the two parameters:

$$C_{out} = C_{in}\big(1 - \alpha(x_i)\big) + c(x_i)\alpha(x_i)$$

   where $\mathbf{C_{out}}$ is the outgoing intensity/color for voxel X along the ray and $\mathbf{C_{in}}$ is the incoming intensity for the voxel.

4. **Compositing.** After all sampling points have been shaded, they are composited along the ray of sight, resulting in the final colour value for the pixel that is currently being processed.

Figure 15: Fluoroscopy image in the application at Left) 0° and Right) 30°.

Once the user has performed the percutaneous access to the kidney, he is able to freeze the puncture needle to observe and evaluate its proximity to the target point. For a better understanding of the internal anatomy and initially simplifying the procedure, the trainee can exploit one of the classes of *LACE Library*: LACE_CuttingPlane. By instantiating an object of type LACE_CuttingPlane, the shapes in the scene are clipped by a plane that changes its position and orientation according to the movements of the haptic device, that are visually reflected by the graphic cursor.

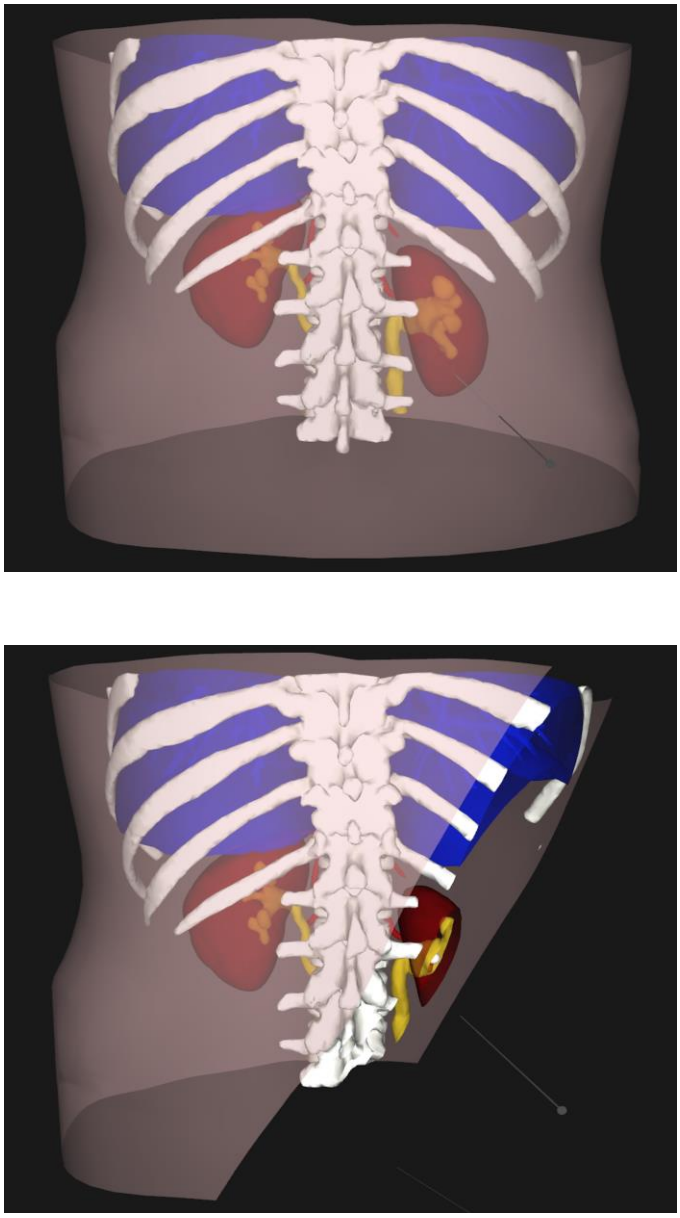

Figure 16: Clipping plane feature of the application.

The 3D models are draggable, and can be translated and rotated by pressing a button on the haptic device: the user is able to freely move the objects in the virtual environment, therefore always obtaining the desired view of the scene.

Stereoscopic view

The stereoscopic view of the scene was implemented by creating a stereo-pairs in the off-axis projections method [44]: the two views are perspective projections of the

virtual environment with parallel cameras. The stereoscopic visualization compensates for the loss of depth perception occurring when 3D shapes are rendered on a 2D computer screen: to overcome this limitation, the user is required to run the application on a 3D monitor that supports the side-by-side mode, and interact with the screen with proper 3D glasses.

To render a stereo pair, one needs to create two images, one for each eye in such a way that when independently viewed they will present an acceptable image to the visual cortex and it will fuse the images and extract the depth information as it does in normal viewing. If stereo pairs are incorrectly created, the depth perception will be exaggerated or reduced, the image will be uncomfortable to watch, the stereo pairs may not fuse at all and the viewer will see two separate images. The off-axis projection method introduces no vertical parallax and is therefore creates the less stressful stereo pairs. Note that it requires a non-symmetric camera frustum, this is supported by some rendering packages, in particular, OpenGL, and it is therefore included in Visualization Library.

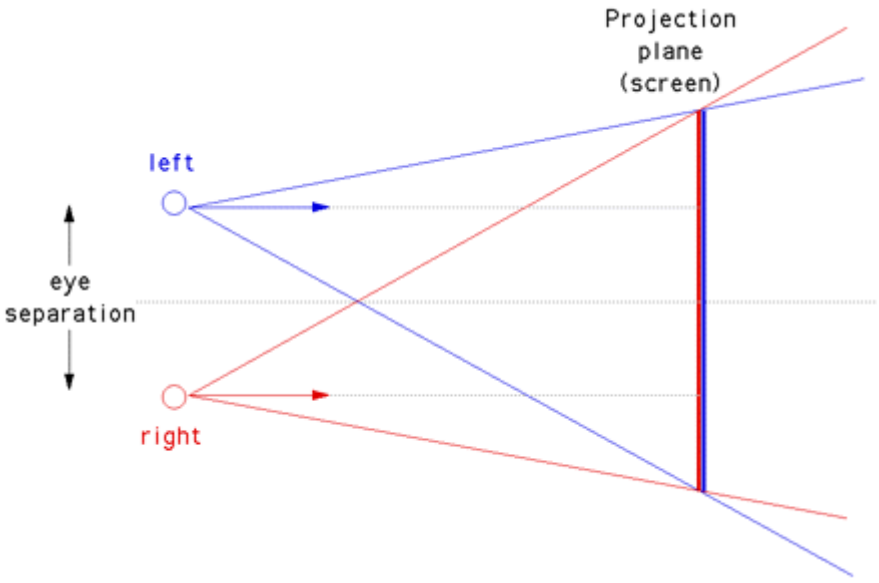

Figure 17: Scheme of the implementation of the off-axis projection method [from [44]]

Camera is defined by its position, view direction, up vector, eye separation, distance to zero parallax and the near and far cutting planes. Position, eye separation, zero parallax distance, and cutting planes are most conveniently specified in model coordinates, direction and up vector are orthonormal vectors. In order not to burden the

operators with multiple stereo controls one can usually just internally set the eye separation to 1/30 of the zero-parallax distance, this will give acceptable stereoscopic viewing in almost all situations and is independent of model scale.

In *LACE Library*, the graphics visualization is rendered at 60 Hz (30 Hz for the left and the right views when the stereo modality is active).

4.3.4 Haptics rendering

The haptic effects that were implemented in the application could be divided in two groups: shape-related effects are related to the material properties of the objects, while event-related effects are activated when the haptic device is inside the skin or inside the kidney.

To detect the collisions with the virtual models, the tip of the haptic device was used. The collision detection algorithm used in the application is the proxy-based, based on a spring-damper model. The reaction force is proportional to the penetration depth, defined as:

$$Penetration\ Depth = Haptic\ Device\ Position - Proxy\ Position$$

The proxy is a point which closely shadows the position of the haptic device, and it is constrained to the exterior surfaces of all touchable shapes when the tip of the device in inside them. The haptic rendering engine continuously updates the position of the proxy. While the actual position of the haptic device may be inside an object, the proxy will always be outside. The detection of a collision is the basis for both the classes of haptic effects, as the onset of a specific feedback is caused by the interaction of the device with the rendered shapes. A graphical representation of the spring-damper model used for the proxy-based method for collision detection is presented in Figure 18.

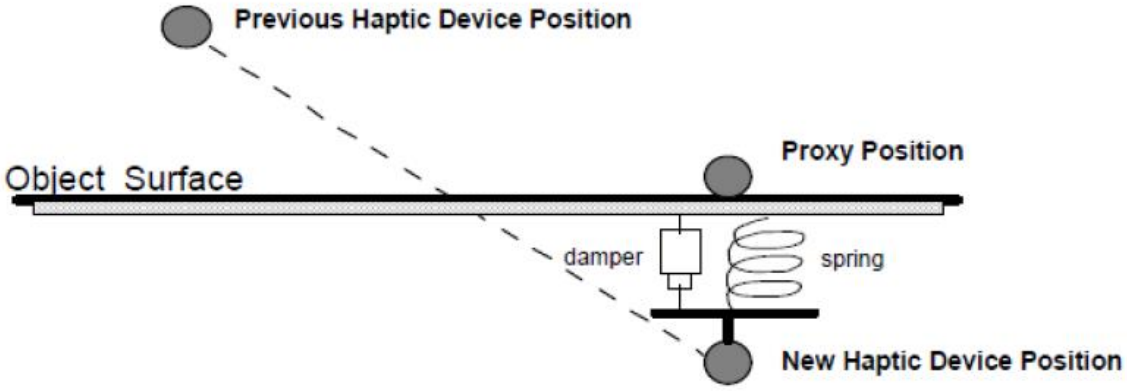

Figure 18: Proxy- based collision detection algorithm (from [45])

Shape-related haptic effects

Each 3D models visible in the scene has specific haptic properties of stiffness, damping, static and dynamic friction and pop through. The GUI allows the user to pick a particular shape within the scene and change its material properties, whose values are absolute numbers in a range between 0 and 1. When a collision is detected, the proxy algorithm computes the forces to be sent to the haptic device depending on the object material properties and on the penetration depth, therefore on the disparity between proxy position and haptic device position. The initial values of the haptic properties for the 3D models are reported in Table 1.

	Skin	Bones	Lungs	Kidney	Ureters	Aorta	Spleen
Stiffness (A.V)	0.4	1	0.5	0.4	0.2	0.2	0.4
Pop-Through (A.V.)	0.05	0.7	0.5	0.05	0.2	0.2	0.5
Damping (A.V.)	0.1	0.5	0	0.1	0	0	0
Friction (A.V.)	0	0.7	0	0	0	0	0

Table 1: Initial values of the haptic features for the 3D models.

Event-related haptic effects

The haptic effects belonging to this second class are activated by the occurrence of certain events in the virtual environment. When the tip of the needle collides with the front surface of the skin with an applied force greater than the pop through value of the shape, the instrument gets inside of the object, triggering a first bunch of tactile stimuli. In this situation, a constant damping effect is perceived by the user, and the so called haptic fulcrum point effect is generated.

The haptic fulcrum point effect simulates the sensation that is experienced when the surgeon penetrates a tissue with a pointed instrument: he/she is free to move the needle in the direction of the incision, back and forth, but not to drive it laterally without feeling the constraint of the surrounding tissue. When the force applied on the skin exceeds its resistance, the proxy position of the tip of the needle is stored, as that is the location of the fulcrum point **f**. In the servo-loop thread the position and the orientation of the haptic device are computed in each frame, and the line **l** passing by the fulcrum point with the same orientation of the stylus is generated. By considering the projection of the current stylus position **p** onto the fulcrum line, the desired stylus position **p'** is then calculated. The force perceived through the haptic device is computed as the distance between **p** and **p'** multiplied by a pre-set gain.

The algorithm for implementing the fulcrum point effect is reported below:

//invocation of the function

```
	void HLCALLBACK myComputeForce(HDdouble force[3], HLcache* cache,
void* userLaceClass)
	{
```

//setting of a constant force feedback

```
		PCA::Omni->setConstantForce(hduVector3Dd (0,1,0), 0.1);
		if (PCA::flagS)  //to check the position of the proxy
		{
			PCA::flagS = false;
			hlCacheGetDoublev(cache, HL_PROXY_POSITION,
PCA::fulcrumPointSkin);
```

```
        }
        if (!(PCA::popS))
```
//obtain the position of the proxy and store it in a cache
```
        {
                hlCacheGetDoublev(cache,HL_PROXY_POSITION, PCA::pos);
                hlCacheGetDoublev(cache,HL_PROXY_ROTATION, PCA::ori);
```
//obtain the vector field of the orientation of the proxy
```
                hduQuaternion unitVector(0,hduVector3Dd(0,0,1));
```
//unit vector of direction with complex conjugates
```
                unitVector = PCA::ori.conjugate()*unitVector*PCA::ori;
                PCA::p0 = PCA::fulcrumPointSkin;
                PCA::p1 = PCA::p0+unitVector.v();
```
//identification of a line within the vector
```
                hduLine <float> line(PCA::p0,PCA::p1);
```
//projection of the new position of the haptic device on the line
```
                hduVector3Dd newPos = line.project(PCA::pos);
```
//force computation $\overline{Force(n)} = \left(\overline{Position\ (n)} - \overline{Position(n-1)}\right) \times Gain\ [N]$
```
                hduVector3Dd force = (newPos-PCA::pos)*PCA::gainS;
                float length= (float) force.magnitude();
```
//capping of the force to not exceed the maximu of 3.3N
```
                if (length> PCA::maxForceS)
                      {
                            force.normalize();
                            force*= PCA::maxForceS;
```
//accumulation of the generated force and storage to be used in the next loop
```
                hdGetDoublev(HD_CURRENT_FORCE,PCA::accumForce);
```

```
                hduVector3Dd newForce = force+PCA::accumForce;
                HDdouble nominalMaxForce;
                hdGetDoublev(HD_NOMINAL_MAX_FORCE, &nominalMaxForce);
                float forceLength= (float) newForce.magnitude();
                if (forceLength> nominalMaxForce)
                      {
                      newForce.normalize();
                      newForce*= nominalMaxForce;
                      }
}
```

A visual representation of the haptic fulcrum point effect computation is showed in Figure 19.

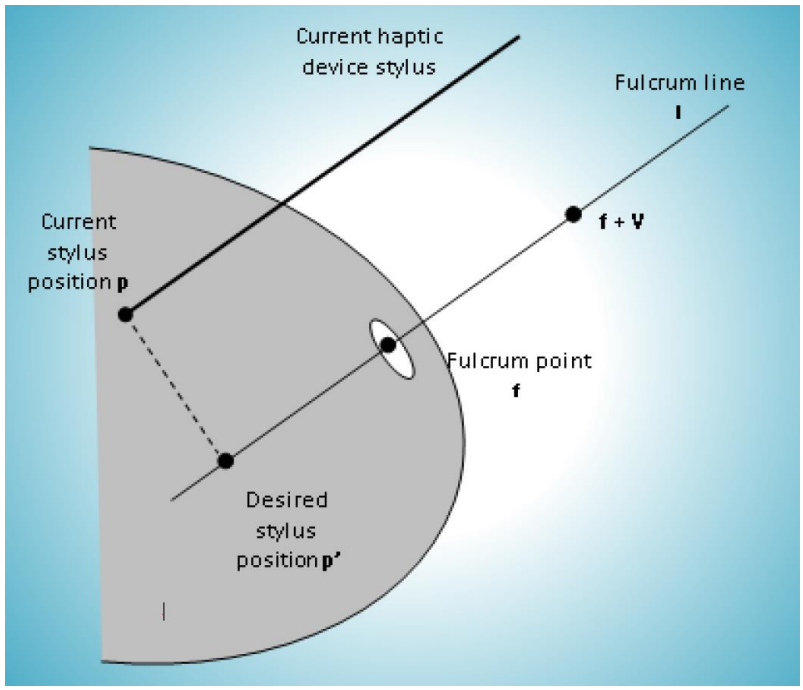

Figure 19: Haptic fulcrum point effect.

A second group of event-related haptic effects is triggered when the needle soaks into the surface of the kidneys: in this case, that is clearly subsequent to the

penetration of the skin, a constant friction and an increased damping stimulus are added to the haptic fulcrum point effect.

When the needle is taken out of the objects with an applied force greater than the pop through value of the back surfaces of skin and kidneys, these haptic effects are disabled.

The GUI allows the user to redefine the value of the gain, as to make the perceived constraint as similar as possible to the sensation of tissue perforation from the surface of the skin to the kidneys.

A general overview of how and when the haptic feedbacks are triggered is represented in the flowchart in Figure 20.

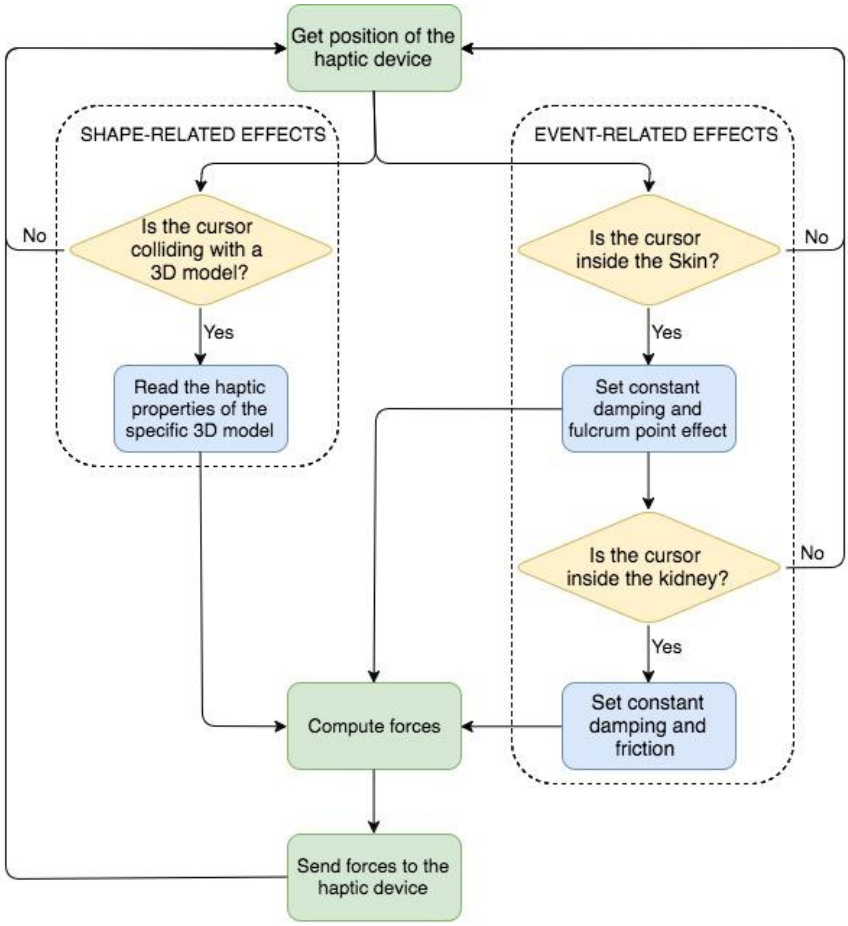

Figure 20: Haptics rendering flowchart.

4.3.5 Graphical user interface

The need for a graphical user interface (GUI) derives from the necessity of managing the graphic and haptic effect of the objects in the scene, such as transparency and haptic material properties, without manually resetting the code and restarting the application. To give the user the possibility to easily customize his/her settings, a GUI was implemented, and as *LACE Library* is a C++ middleware relying on GLUT to handle all system-dependent issues, it was opted toward the GLUI User Interface Library.

GLUI [46] is a GLUT-based C++ library which provides controls to OpenGL applications, to make the user able to interact with the program. It is window-system independent, and its ease of use and integration with the pre-existent environment justified the choice. The tools available with GLUI are sliders, scrollbars, buttons and checkbox: the graphic interface developed for the application is composed on several scrollbars for tuning the transparency, the stiffness, the damping, the friction and the pop through values for the 3D models. It also includes additional sliders for setting the brightness and the upper and lower thresholds of the transfer function used to render the fluoroscopy image, and a panel to let the trainee choose his/her target between the six that were predefined. In the case of a new user, the default parameters are given to the scene at the beginning of the application: once he/she modifies the graphic and haptic properties of the objects, the new values are stored into a text file, as they could be reset instead of the standard ones when the same person will run the application the next time.

4.3.6 Performance evaluation

The main advantages of virtual reality based simulator is their capability of providing performance reports at the completion or during the task. Besides a qualitative assessment the simulator should therefore be able to offer a quantitative evaluation of the user's skill, to assess the eventual improvement of the trainees over time and consequently state the effectiveness of the training with this tool.

At the completion of the task, as already mentioned before, the user freezes the puncture needle: at this point, he/she is able to both visually explore the anatomy and

the location of the instruments with respect to the target and to get some quantitative feedbacks of his/her task.

One of the main drawbacks of performing percutaneous surgery under radiographic guidance is the amount of radiation the patient and the personnel in the operative room are exposed to. As previously seen in Chapter 2, fluoroscopy can result in relatively high radiation doses, especially for complex procedures like PCA. To minimize the exposure to radiation, fluoroscopy should always be performed for the shortest time necessary with an adequate exposure: physicians who are approaching this surgery should practice on keeping the fluoroscopy time as lower as possible. In the implementation of the simulator, the total time of fluoroscopy usage is tracked and displayed on the screen, as an indication of the ability of the user to puncture the kidney and access the calix by limiting the amount of radiation.

Besides the fluoroscopy time, it is necessary for the surgeon to reach the calices without compromising other structures and avoiding multiple punctures: the success of the procedure is determined by a correct access to the kidney and the its collecting system. For this reason, a bunch of data are collected during the task that reflect the trainee's performance. With the proxy-based collision detection method illustrated in Figure 18, and with a specific built-in function of QuickHaptics, a counter for all the interactions with the virtual models in the scene has been implemented. At the end of the task, all the quantitative data elaborated from the simulator are saved in a text file that is accessible from the apprentice and from the supervisor of the training. The process is completely automatized and allows the user to keep a track of the improvements in the task performing time after time.

The performance indicators that are stored are:

- the duration of the task, intended as the time from the first fluoroscopy shot and the freezing of the needle, expressed in seconds;
- the fluoroscopy time, measured with a time counter during the period when the live fluoroscopy imaging is kept on, expressed in seconds;
- the distance from a desired target, placed in the left renal collecting system, and calculated in centimetres at the freezing of the needle with the Euclidean formula for the distance between two points in the 3D

space, the ideal target P (p_x, p_y, p_z) and the tip of the virtual needle Q (q_x, q_y, q_z);

$$Distance = \sqrt{(p_x - q_x)^2 + (p_y - q_y)^2 + (p_z - q_z)^2}$$

- the undesired contacts with spleen, lungs, spine and major vessels, intended as the number of time the tip of the virtual needle collided with the virtual models in the scene.

Chapter 5

5. Experimental protocol and results

The application presented in this thesis was developed on a workstation available at the University of Illinois at Chicago. The majority of tests were performed at Politecnico di Milano, where the available setup was slightly different from the one used for the development phase. The main features of the two systems are reported in Table 2. Beside a better setup as for processors and memory features, the monitor we had at our disposal at Politecnico di Milano did not allow users for stereoscopic visualization.

	POLIMI	UIC
Processor	Intel Core i7 - 6800K CPU 3.4GHz	Intel Core i5 - 2500K CPU 3.3GHz
RAM	16GB	8GB
GPU	NVIDIA TITAN Xp	NVIDIA Quadro K6000
Stereoscopic display	No	Yes
Haptic device	3D System Touch™ 3D Stylus	SensAble Phantom OMNI

Table 2: Features of the experimental setup at Politecnico di Milano and at UIC

We recruited medical students from Ospedale “Sacco” in Milano. In total, 15 medical students (21-24 years old) participated in this study, with no previous practical experience with the procedure itself, but strong knowledge of the human anatomy and theoretical base of percutaneous surgery.

Each trainee was solicited to access the collecting system of the virtual left kidney 3D model with a virtual needle, controlled by the haptic device stylus, twice. The learners could freely manipulate the virtual C-arm device to control the time of fluoroscopic exposure and location around the virtual patient anatomy. To make the test as standard as possible, the position of the 3D models was fixed in the scene, with patient in a prone position, slightly inclined (approximately 30°) to present the left side of the back and allow the trainees to access the left kidney. In particular, the participants were asked to:

1. Set the useful projections of the virtual fluoroscopy (0°, 30° and 60° with respect to the horizontal plane);
2. Press and release a button to have visibility of the needle in the fluoroscopy imaging;
3. Insert the virtual needle inside the patient through the skin;
4. Trying as much as possible to avoid undesired contacts with the organs in the scene, in particular spleen and lungs, with the spine and with the aorta;
5. Place the needle inside the left kidney, as close as possible to the target (the centre of the renal pelvis);
6. Press the space bar to freeze the needle in the desired position and independently check their performance: at the end of the task the time (in seconds) of usage of the fluoroscopy, the total time of the procedure (in seconds) and the distance from the target (in centimetres) were displayed;
7. Repeat all the previous steps, with better knowledge of the anatomy of the patient and more confidence with the haptic device.

Study design

None of the participants had previous knowledge about this simulator. Therefore, a brief orientation session about the simulator was offered on how to control the fluoroscopy unit, before proceeding to performing the task. However, participants were not allowed to practice on the simulator prior to starting their session.

After each attempt, the simulator calculated: operative time, fluoroscopy time, distance from the tip of the needle to the ideal target (centres of the renal pelvis), and number of undesired contacts (lesions) to surrounding organs.

Each trainee was then asked to complete a Standard Usability Scale (SUS) test, a simple, ten-item attitude Likert scale questionnaire giving a global view of subjective assessment of usability (range 0-100), and a custom questionnaire to rate their experience with the haptics simulator.

Statistical analysis

Data from the questionnaires and performance reports generated by the simulator were collected and analysed. Descriptive data were presented in terms of medians and quartiles or means and standard error of mean. The Wilcoxon signed-rank test was used to compare data generated by performance reports, as it is advisable when comparing repeated measurements to assess whether their population mean ranks differ. Two tailed p value <0.1 was considered significant.

Figure 21: Test phase with the medical students at Ospedale "Sacco", Milano.

5.1 Quantitative evaluation

There were no statistically significant differences between the first and the second attempt in terms of distance from the target (p=0.76), total time of the procedure (p=0.2), interactions with spleen and lungs (p=0.79 and p=0.017, respectively), while a statistically significant difference in terms of time of fluoroscopy (p=0.05), interactions with the bones (p=0.07) and interactions with major vessels (p=0.07) was highlighted.

Performance indicator	Attempt A	Attempt B
Distance from target (cm)	2.42 ± 0.27	2.61 ± 0.39
Time of fluoroscopy (sec)	102.6 ± 16.6	67.1 ± 9.7
Total time (sec)	116 ± 17.2	83.2 ± 11.2
No. interactions w/ spleen	8.4 ± 3.36	8.9 ± 3.87
No. interactions w/ bones	15.8 ± 3.9	7.7 ± 1.7
No. interactions w/ lungs	46.2 ± 10.8	17.2 ± 6.4
No. interactions w/ vessels	53.1 ± 2.1	25.2 ± 8.5

Table 3: Mean and standard error of performance indicators for attempt A and B.

Performance indicator	Attempt A	Attempt B
Distance from target (cm)	2.6 (1.41-3.25)	2.27 (1.48-3.5)
Time of fluoroscopy (sec)	80.3 (46.3-190.1)	58.4 (34.8-90.4)
Total time (sec)	102.8 (54-190.1)	69.8 (44.3-132.6)
No. interactions w/ spleen	4 (0-8)	1 (0-15)
No. interactions w/ bones	12 (4-25)	6 (4-8)
No. interactions w/ lungs	47 (2-93)	1 (0-31)
No. interactions w/ vessels	54 (2-89)	6 (0-54)

Table 4: Median value of performance indicators for attempt A and B (first-third quartile).

In the present study, medical students performed globally better on the haptics-based simulator in their second attempt rather than in their first one. Specifically, they had significantly shorter fluoroscopy time (102.6 ± 16.6 vs. 67.1 ± 9.7 seconds), total time of procedure (116 ± 17.2 vs. 83.2 ± 11.2), number of interactions with bones (15.8 ± 3.9 vs. 7.7 ± 1.7), lungs (46.2 ± 10.8 vs. 17.2 ± 6.4) and major vessels (53.1 ± 2.1 vs. 25.2 ± 8.5).

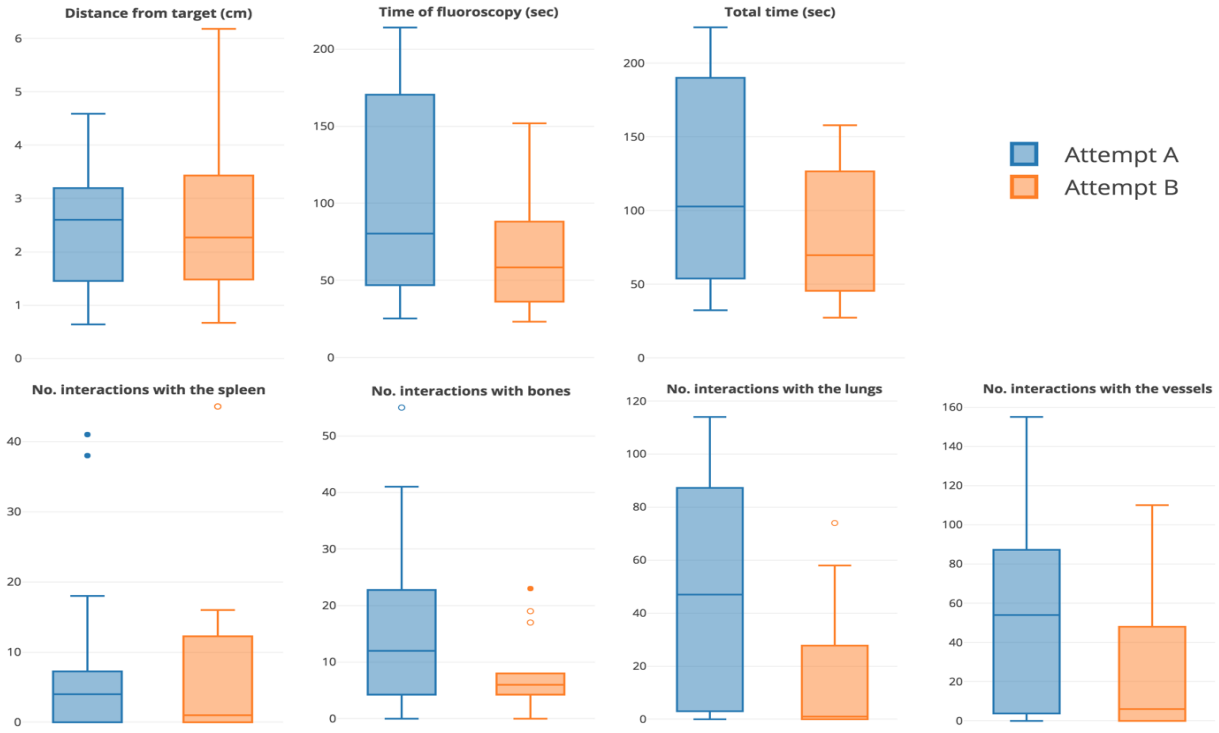

Figure 22: Boxplots of performance indicators between attempt A and attempt B

5.2 Qualitative evaluation

Assessment questionnaire

The questionnaire for the qualitative assessment of the simulator consists of 13 questions, that are either open or multiple choice (whose possible answers are reported in Table 5). The first questions aimed at gathering information about users' medical experience, and their familiarity with percutaneous renal surgery and virtual reality simulations. Questions from 3 to 11 are multiple choice questions that allow urologists to rate their experience with the simulator. The last questions are used to obtain further general feedback. The full questionnaire is included in the Appendix.

1	Not at all
2	Somewhat
3	Fairly
4	Very
5	Extremely

Table 5: Multiple choice answers.

In the pie-chart below are reported the answers to the assessment questionnaire. Despite being a novel technology, the students demonstrated a good attitude and willing to accept the technology as a training tool.

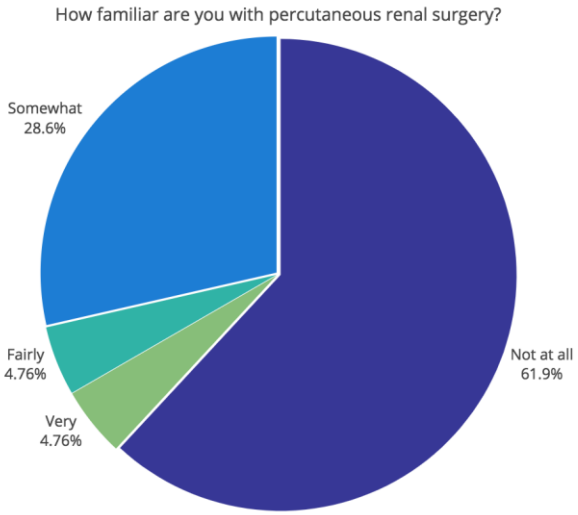

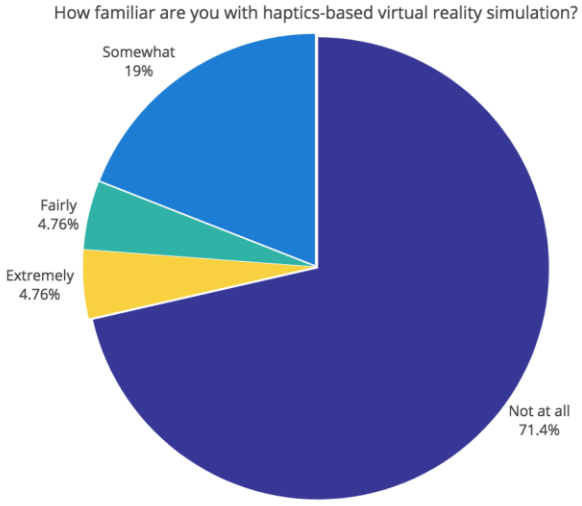

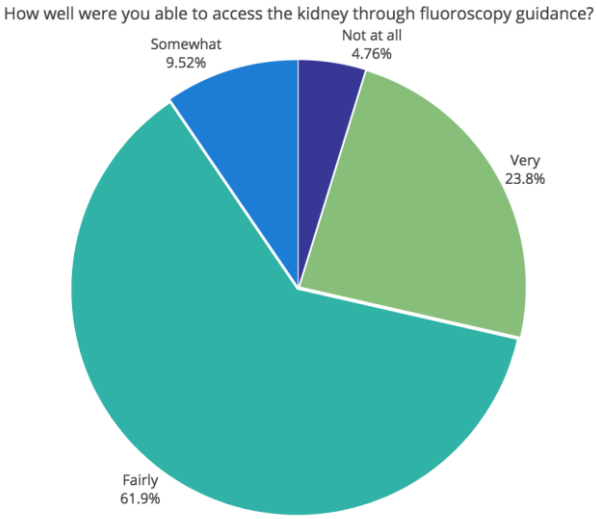

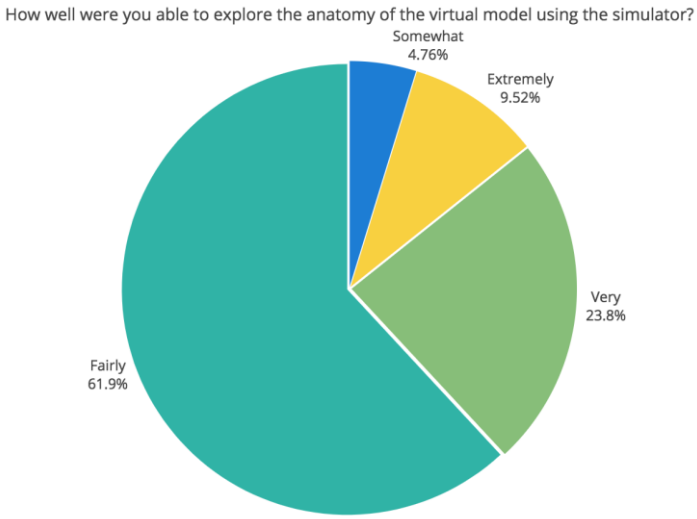

How well were you able to haptically differentiate tissue stiffness of the virtual models?

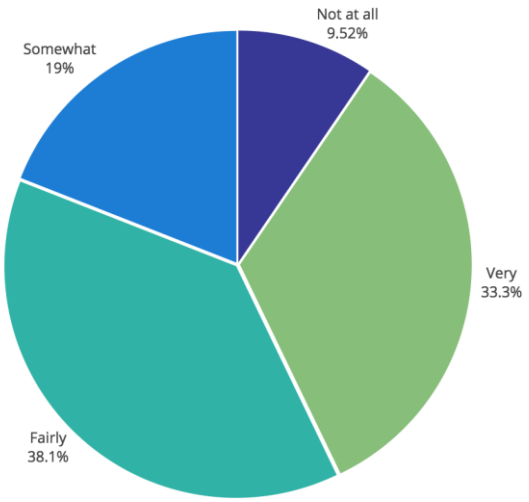

To what extent does tactile feedback feel realistic?

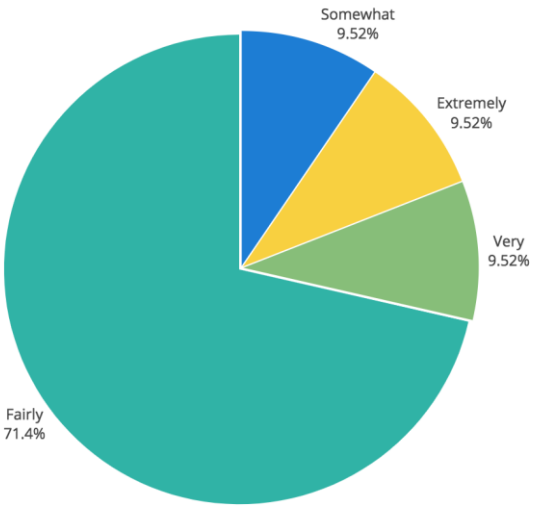

How easily have you learnt how to interact with the simulator?

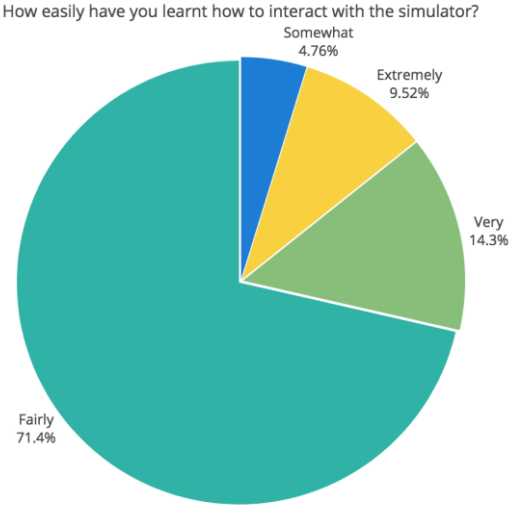

To what extent do you think the simulator would be useful for training in PCA?

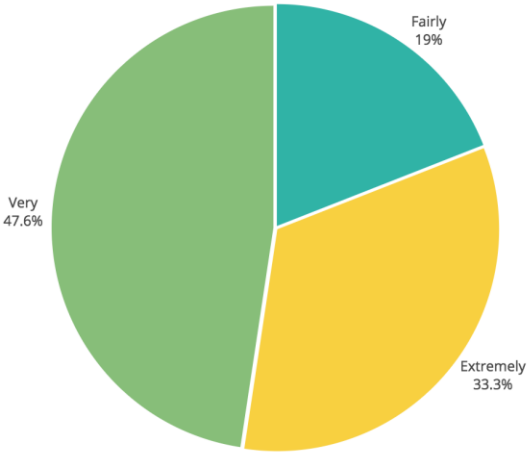

To what extent do you think the correspondence between 3D models and fluoroscopic image is accurate?

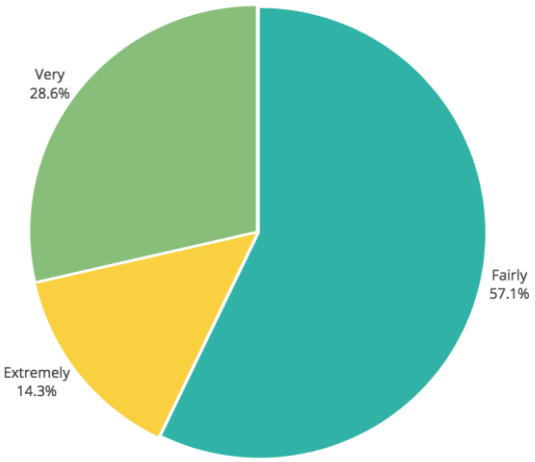

How satisfied were you when using the simulator?

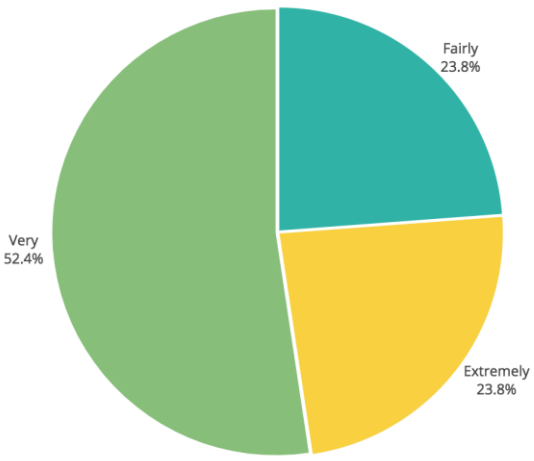

System Usability Scale test

The students were then asked to fill a second questionnaire, called System Usability Scale (SUS). SUS is a simple ten-item scale developed by Brooke et al. [47] which allows to subjectively assess new technology usability. The respondent has to indicate his/her extent of agreement or disagreement to each statement on a 5-point scale (from 1 -Strongly Disagree- to 5 -Strongly Agree-). SUS score is a single number in the range 0-100 that represents a measure of the overall usability of the system being evaluated. In order to compute it, the score contributions from each item have to be summed. Score contributions are defined as the scale position minus 1 for items 1, 3, 5, 7, 9, and as 5 minus the scale position for items 2, 4, 6, 8, 10. In this way, each item's score contribution ranges between 0 and 4. The overall SU value is then obtained by multiplying the sum of scores by 2.5, as reported in the equation below.

$$SUS_{score} = 2.5 \left(\sum_{i=1,3,5,7,9} (q_i - 1) + \sum_{i=2,4,6,8,10} (5 - q_i) \right)$$

The questions from the SUS test are reported in Table 6.

N	Statement
1	I think that I would like to use this system frequently.
2	I found the system unnecessarily complex.
3	I felt very confident using the system.
4	I found the various functions in this system were well integrated.
5	I thought the system was easy to use.
6	I thought there was too much inconsistency in this system.
7	I found the system very cumbersome to use.
8	I would imagine that most people would learn to use this system very quickly.
9	I think that I would need the support of a technical person to be able to use this system.
10	I needed to learn a lot of things before I could get going with this system.

Table 6: System Usability Scale test.

From the questionnaires, we computed an initial global SUS score, by averaging the SUS scores of each participant. The obtained value with the standard error is:

$$SUS_{avg} = 71 \pm 4.6$$

The pie-chart below represent the percentage of the answers to the SUS test.

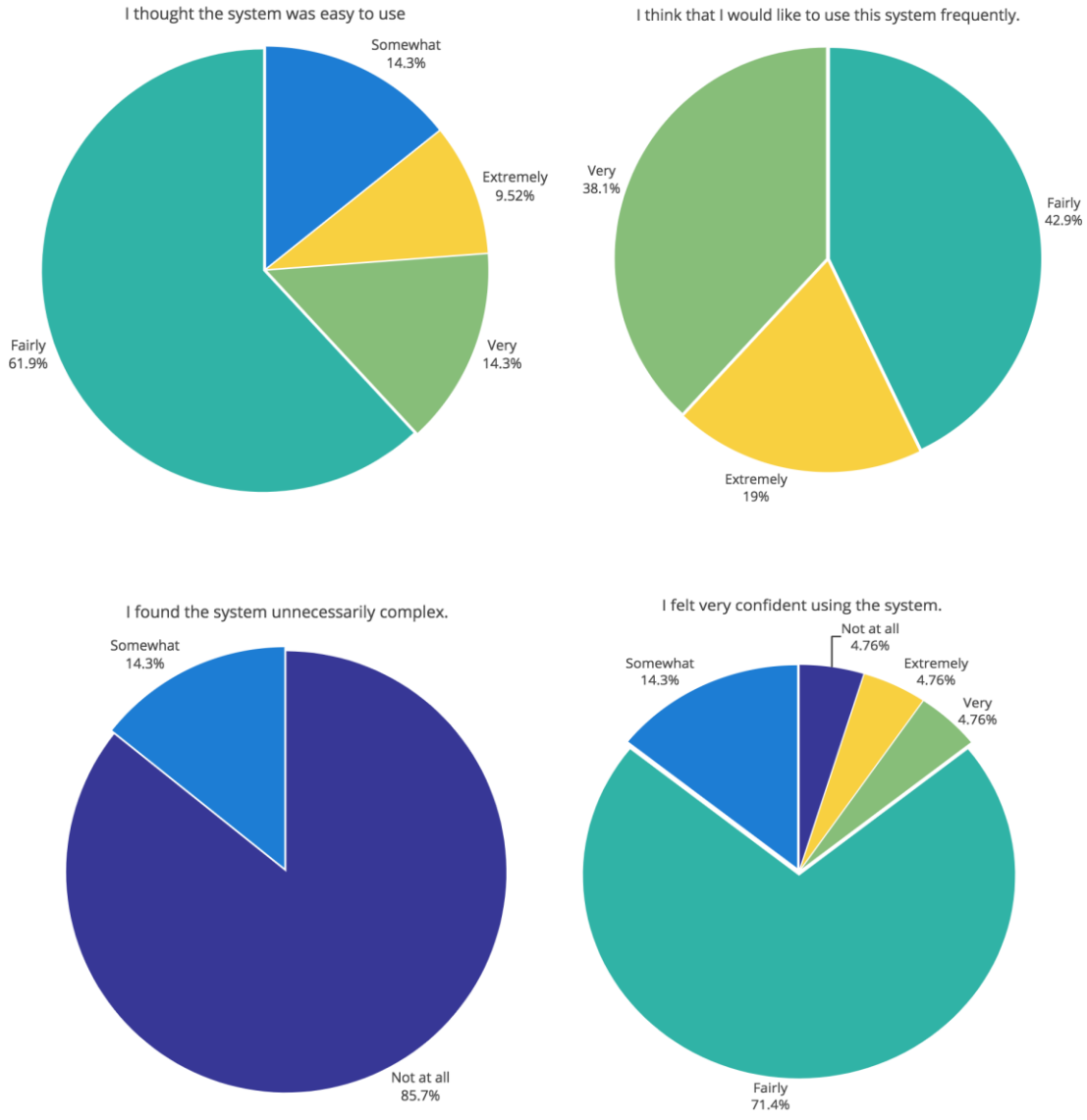

I found the various functions in this system were well integrated.

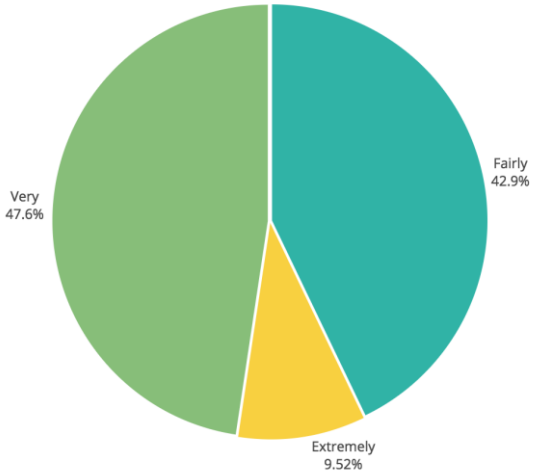

I thought there was too much inconsistency in this system

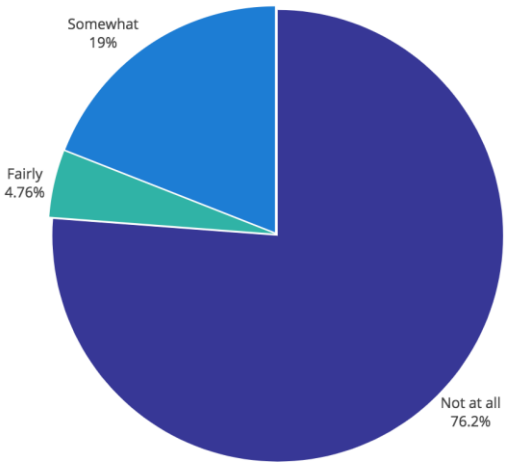

I found the system very cumbersome to use.

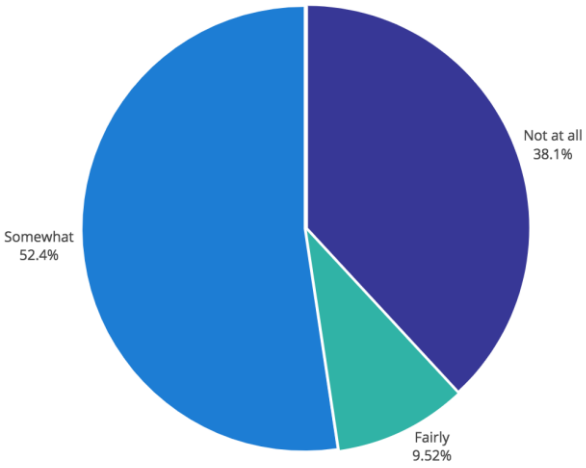

I think that I would need the support of a technical person to be able to use this system.

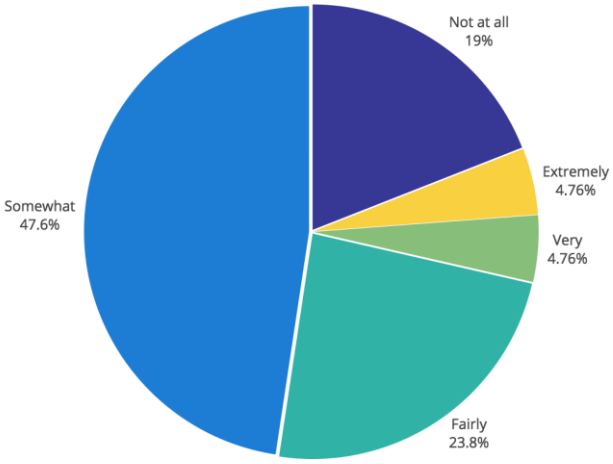

I needed to learn a lot of things before I could get going with this system.

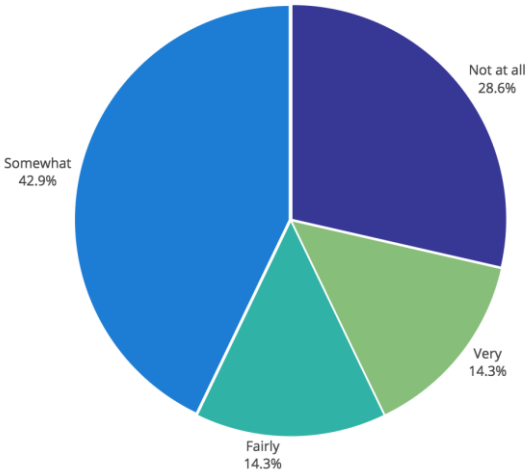

I would imagine that most people would learn to use this system very quickly.

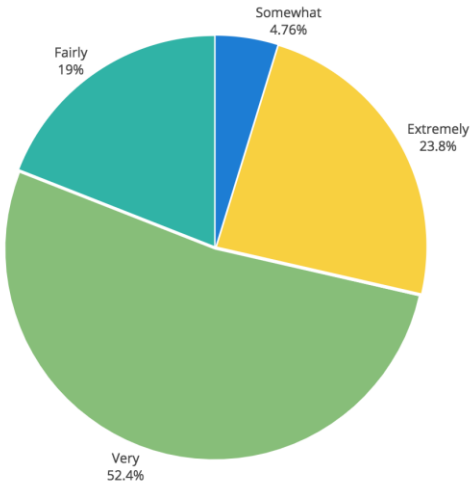

Chapter 6

6. Discussion

The aim of this thesis work was the development and evaluation of a haptics-based simulator for training in percutaneous renal access, and it is addressed to those physician, like urologists and interventional radiologists, that routinely perform percutaneous renal surgery. The acquisition of the necessary skills to obtain a good percutaneous access to the kidney is linked to a steep learning curve, and as PCA is usually done once for each procedure, the trainees are prevented from gaining experience and confidence in the surgery by only attending the operative rooms. Most of the competencies obtained by clinicians are due to situational events, thus the use of simulators can accelerate training in those individuals desiring to be capable in this procedure. A simulator that is able to provide the trainees with competency could diminish the time associated with learning the procedure, and potentially reduce the risks for patients undergoing percutaneous renal surgery as trainees start operating. The application that was developed tends to meet those negatives encountered in other training models found in literature.

Unlike biological bench models with porcine or bovine kidney, it is anatomically accurate, as the 3D models are segmented and extracted from real patient's images. The ethical concerns of using parts or entire animals are obviously avoided. Those models, as well as non-biological prototypes, are also subject to degradation and have to be replaced after several repetitions of the procedure. With the virtual simulator, the task can be performed an indefinite number of times without redefining the experimental set-up, saving resources in terms of cost of the materials and effort in the continuous reset of the model.

The application allows to perfectly emulate the fluoroscopy guidance by keeping a radiation-free environment: the trainee is therefore able to practice in safe conditions and to acquire the necessary skills in managing a C arm unit at the same time.

The current virtual reality simulator used for training in PCA, i.e. the PERC Mentor™, is extremely high-priced and its widespread use is consequently limited; furthermore, it is not provided with reliable tactile feedbacks. The haptics-based surgical simulator was implemented with a reasonably low-cost hardware, the Touch™ 3D Stylus, while the software is composed by four C++ libraries: the workstation is constituted by a haptic device, a computer running with a Windows operative system and a 3D monitor to exploit the stereoscopic visualization, making the global simulator easily accessible.

The application has demonstrated good performances: the efficiency of *LACE Library* allows to have a stable haptic effect despite the high computational load due to the heavy dataset and the well-defined 3D models in the graphics rendering. There are no perceivable delays between the actual movement of the haptic stylus and the displacement of the needle on the screen.

Preliminary evaluation at University of Illinois at Chicago

We asked some experienced urologists who collaborate with the Mixed Reality Lab at UIC to qualitatively assess the usefulness of the application and test its realism in terms of graphics and haptics rendering. They were given the possibility to tune the haptic properties of the shapes and customize the simulator with features based on their applied expertise. The newly-defined parameters were then applied as default to the scene.

One of the urologists underlined that the majority of the interventional radiologists who routinely perform this procedure do not rely on fluoroscopic imaging in the preliminary phase of the renal access, but only on US guidance for a better visualization of the surrounding soft tissues: he therefore suggested the integration of both the imaging method for a more complete training instrument.

There was a general recognition of the potential impact of the application as a training tool for learning the basic steps to obtain PCA: the haptic feedbacks triggered

when puncturing the skin and penetrating the fascia was considered convincing, as well as all the haptic properties related to the 3D models.

The fluoroscopy guidance was tested to access the calices, and resulted in being highly accurate and precise: by applying one of the approaches shown in *Chapter 2.3.4*, the urologists were actually able to reach the desired target, with a perfect match of the position of the needle in the radiographic image and in the 3D models.

The great value of the simulator was globally acknowledged for the training of urologists, which in their residency need to learn how to manage a C arm unit and process in their mind a three-dimensional reconstruction of the internal human anatomy from the two-dimensional information of the fluoroscopy image.

Test phase at Ospedale "Sacco" in Milano

Data from performance reports reveal a general improvement of the KPIs in the second repetition of the task. All the medians of the performance indicators are lower in attempt B, while only the interactions with the spleen and the distance from target increased when considering the mean value.

On the other hand, a wider range of values emerged from the results in attempt B: the students rapidly gained confidence with the haptic device and the simulator, and while in their first approach they seemed to be cautious, in their second attempt they performed the task faster, shortening the total time but extending the range of the undesired contacts with the 3D models.

The global scope of the students included in the study was a decrease of the fluoroscopy time with respect to the total time of procedure from attempt A to attempt B, and as this can be seen from the distribution of data in Figure 22, it is proved by a reduction of the correlation coefficient between the indicators (0.98 vs. 0.83).

The last evaluation we performed, with the System Usability Scale, allows us to get a preliminary impression about the general usability of the simulator. The mean SUS score we obtained is of 71 out of 100. According to the study carried out by Bangor et al. in [48], the system has an overall "Good" usability.

Chapter 7

7. Conclusion

This work describes the implementation and the test phase of a haptics-based surgical simulator for percutaneous renal access. The application is built upon an efficient and novel C++ based software, *LACE Library*, which has been created by the candidate in collaboration with three colleagues from the Department of Bioengineering at the UIC. This platform has demonstrated to succeed in obtaining an optimal distribution of the computer load between high-performance 3D graphics and real-time haptics rendering. The development of *LACE Library*, and its continuous updating in the next future, provides a valuable tool for those interested in creating virtual and augmented reality-based application.

The achieved simulation integrates both visual and haptic information on patient-specific 3D models of the kidney and its collecting system, spine, skin, lungs and vessels extracted from a real volumetric dataset. It enables to perform a renal puncture under fluoroscopy guidance by keeping a radiation-free environment. The haptic sensation implemented relies on the feedbacks given by expert surgeons which routinely perform percutaneous renal access.

This simulator may represent an important resource for enhancing the current training of Interventional Radiology and Urology residents: our innovative haptics-based VRS showed the potential to improve hand-eye coordination, shorten the learning curve for PCA, allowing training in a patient-safe and radiation-free environment. The results of questionnaires proved it was well appreciated. Since this is a pilot study, further randomized clinical trials enrolling high samples of trainees are necessary to validate our preliminary results and support the diffusion of our simulator.

7.1 Future research and developments

Several feedbacks were given from expert urologists after the preliminary evaluation, regarding the improvements and modifications to the content of the simulator:

1) the design of a dynamic application, by taking into consideration the displacement of the organs due to respiration. This could be achieved with the segmentation of a dataset from a 4D CT scanning, to track in particular the movement of the kidneys along the whole respiratory cycle;
2) the integration of the US guidance to provide the trainees with an exhaustive training tool for percutaneous renal access. The combination of US and fluoroscopic guidance is the preferable method to have at the same time a good visibility of the soft tissues and to see with an optimal resolution the needle and the target calix;
3) the inclusion of an automated segmentation algorithm in the program itself, to give the user the possibility to extract and visualize 3D models by loading the volumetric dataset in the application and avoiding the preliminary phase of processing the meshes;

It is undeniable that a more sophisticated hardware would allow to obtain higher performances, both in terms of graphic and haptic accuracy. A head mounted display can be incorporated in the application to achieve a better 3D view of the scene, as well as a 6 degrees of freedom haptic device can be used to provide a more complete force feedback based on both forces and torques. At the same time, these integrations would affect the costs of the overall workstation.

Lastly, *LACE Library* should be extended and generalized, to provide those interested in medical simulation with a precious tool for creating application in a virtual and augmented reality-based environment. A better interaction among the basic libraries could be obtained so that the platform will gain more consistency, and additional ones should be added, such as a dynamic engine for simulating objects' dynamics and instruments for the recording and generation of sounds.

Appendix A

Assessment Questionnaire

1. What is your actual position?
2. How familiar are you with percutaneous renal surgery?
3. How familiar are you with haptics-based virtual reality simulation?
4. How well were you able to access the kidney through fluoroscopic guidance?
5. How well were you able to explore the anatomy of the virtual model using the simulator?
6. How well were you able to haptically differentiate tissue stiffness of the virtual model?
7. To what extent does tactile feedback feel realistic?
8. How easily have you learnt how to interact with the simulator?
9. To what extent do you think the simulator woud be useful for training in PCA?
10. To what extent do you think the correspondence between 3D model and the fluoroscopic image is realistic?
11. How satisfied were you when using the simulator?
12. Which features would you add to the simulator?
13. Comments and suggestions.

Appendix B

This thesis work involved the participation of physicians and medical students in the evaluation and testing of a haptics-based simulator for training in percutaneous renal access. The protocol for this study was approved by Institutional Review Board (IRB) at the University of Illinois at Chicago **Approval 2017-0163**

Bibliography

[1] F. H. Netter, *Atlas of human anatomy*, 3rd ed. 2003.

[2] S. S. Salami, Z. Okeke, and A. D. Smith, "Percutaneous renal access: a historical perspective," in *Percutaneous Renal Surgery*, 2013, pp. 1–5.

[3] M. R. Hotston, S. Mathur, and F. X. Keeley, "Percutaneous Management of Transitional Cell Cancer (Percutaneous Resection of Tumor)," in *Percutaneous Renal Surgery*, 2013, pp. 173–180.

[4] N. L. Miller, B. R. Matlaga, and J. E. Lingeman, "Techniques for Fluoroscopic Percutaneous Renal Access," *J. Urol.*, vol. 178, no. 1, pp. 15–23, 2007.

[5] G. Sharma and A. Sharma, "Determining site of skin puncture for percutaneous renal access using fluoroscopy-guided triangulation technique.," *J. Endourol.*, vol. 23, no. 2, pp. 193–195, 2009.

[6] G. R. Sharma, P. N. Maheshwari, A. G. Sharma, R. P. Maheshwari, R. S. Heda, and S. P. MAheshwari, "Fluoroscopy guided percutaneous renal access in prone position," *World J. Clin. Cases*, vol. 3, no. 3, p. 245, 2015.

[7] J. D. Watterson, S. Soon, and K. Jana, "Access Related Complications During Percutaneous Nephrolithotomy: Urology Versus Radiology at a Single Academic Institution," *J. Urol.*, vol. 176, no. 1, pp. 142–145, 2006.

[8] Y. A. Noureldin and S. Andonian, "Simulation for Percutaneous Renal Access: Where Are We?," *J. Endourol.*, vol. XX, no. Xx, 2016.

[9] L. Hammond, J. Ketchum, and B. F. Schwartz, "a New Approach To Urology Training:: a Laboratory Model for Percutaneous Nephrolithotomy," *J. Urol.*, vol. 172, no. 5, pp. 1950–1952, 2004.

[10] Y. Zhang *et al.*, "Novel Biologic Model for Percutaneous Renal Surgery Learning and Training in the Laboratory," *Urology*, vol. 72, no. 3, pp. 513–516, 2008.

[11] F. Imkamp, C. von Klot, U. Nagele, and T. R. W. Herrmann, “New ex-vivo organ model for percutaneous renal surgery,” *Int. Braz J Urol*, vol. 37, no. 3, pp. 388–394, 2011.

[12] M. M. Abdallah, S. M. Salem, M. R. Badreldin, and A. A. Gamaleldin, “The use of a biological model for comparing two techniques of fluoroscopy-guided percutaneous puncture: A randomised cross-over study,” *Arab J. Urol.*, vol. 11, no. 1, pp. 79–84, 2013.

[13] P. Kallidonis *et al.*, “Modular training for percutaneous nephrolithotripsy: The safe way to go,” *Arab J. Urol.*, vol. 13, no. 4, pp. 270–276, 2015.

[14] F. Bruyère, C. Leroux, L. Brunereau, and P. Lermusiaux, “Rapid prototyping model for percutaneous nephrolithotomy training.,” *J. Endourol.*, vol. 22, no. 1, pp. 91–96, 2008.

[15] Y. Zhang, C. F. Yu, S. H. Jin, N. C. Li, and Y. Q. Na, “Validation of a novel non-biological bench model for the training of percutaneous renal access,” *Int. Braz J Urol*, vol. 40, no. 1, pp. 87–92, 2014.

[16] B. W. Turney, “A new model with an anatomically accurate human renal collecting system for training in fluoroscopy-guided percutaneous nephrolithotomy access.,” *J. Endourol.*, vol. 28, no. 3, pp. 360–3, 2014.

[17] “PERC Mentor | Simbionix.” [Online]. Available: http://simbionix.com/simulators/perc-mentor/. [Accessed: 22-Mar-2017].

[18] B. E. Knudsen *et al.*, “A Randomized, Controlled, Prospective Study Validating the Acquisition of Percutaneous Renal Collecting System Access Skills Using a Computer Based Hybrid Virtual Reality Surgical Simulator: Phase I,” *J. Urol.*, vol. 176, no. 5, pp. 2173–2178, 2006.

[19] S. Mishra *et al.*, “Validation of virtual reality simulation for percutaneous renal access training.,” *J. Endourol.*, vol. 24, no. 4, pp. 635–40, 2010.

[20] A. G. Papatsoris *et al.*, “Use of a virtual reality simulator to improve percutaneous renal access skills: A prospective study in urology trainees,” *Urol. Int.*, vol. 89, no. 2, pp. 185–190, 2012.

[21] Y. Zhang, C. F. Yu, J. S. Liu, G. Wang, H. Zhu, and Y. Q. Na, “Training for percutaneous renal access on a virtual reality simulator,” *Chin. Med. J. (Engl).*, vol. 126, no. 8, pp. 1528–1531, 2013.

[22] “Haptic products | Geomagic.” [Online]. Available: http://www.geomagic.com/en/. [Accessed: 26-Mar-2017].

[23] “CAE NeuroVR Neurosurgical Simulator | CAE Healthcare.” [Online]. Available: https://caehealthcare.com/surgical-simulation/neurovr. [Accessed: 28-Mar-2017].

[24] “LapSim | Surgical Science.” [Online]. Available: http://www.surgical-science.com/lapsim-the-proven-training-system/. [Accessed: 28-Mar-2017].

[25] “ImmersiveTouch Inc.” [Online]. Available: http://www.immersivetouch.com/. [Accessed: 28-Mar-2017].

[26] K. L. Stern, M. D. Tyson, H. M. Abdul-Muhsin, and M. R. Humphreys, “Contemporary Trends in Percutaneous Nephrolithotomy in the United States: 1998-2011,” *Urology*, vol. 91, pp. 41–44, 2016.

[27] C. F. Ng, “Training in percutaneous nephrolithotomy: The learning curve and options,” *Arab J. Urol.*, vol. 12, no. 1, pp. 54–57, 2014.

[28] O. Traynor, “Surgical training in an era of reduced working hours,” *Surgeon*, vol. 9, no. SUPPL. 1, pp. S1–S2, 2011.

[29] S. Faddegon and M. S. Pearle, “Epidemiology of Large Renal Stones and Utilization Patterns of Percutaneous Nephrolithotomy,” in *Percutaneous Renal Surgery*, 2013, pp. 23–30.

[30] P. A. Yushkevich *et al.*, “User-guided 3D active contour segmentation of anatomical structures: Significantly improved efficiency and reliability,” *Neuroimage*, vol. 31, no. 3, pp. 1116–1128, 2006.

[31] “itk-SNAP.” [Online]. Available: http://www.itksnap.org/pmwiki/pmwiki.php. [Accessed: 08-Apr-2017].

[32] “OsiriX | DICOM Image Library.” [Online]. Available: http://www.osirix-viewer.com/resources/dicom-image-library/. [Accessed: 09-Apr-2017].

[33] “ParaView.” [Online]. Available: http://www.paraview.org/. [Accessed: 08-Apr-2017].

[34] “3ds Max | 3D Modeling, Animation and Rendering Software | Autodesk.” [Online]. Available: http://www.autodesk.com/products/3ds-max/overview. [Accessed: 08-Apr-2017].

[35] “Touch Haptic 3D Stylus.” [Online]. Available:

http://www.geomagic.com/en/products/sculpt/touch/. [Accessed: 02-Apr-2017].

[36] "OpenHaptic Toolkit Overview." [Online]. Available: http://www.geomagic.com/it/products/open-haptics/overview. [Accessed: 15-Apr-2017].

[37] "Bosi M.: Visualization Library." [Online]. Available: http://visualizationlibrary.org/docs/2.0/html/index.html. [Accessed: 02-Apr-2017].

[38] A. Faso, "Haptic and Virtual Reality Surgical Simulator for Training in Percutaneous Renal Access," University of Illinois at Chicago, 2017.

[39] L. Rapetti, "Virtual reality navigation system for prostate byopsy," University of Illinois at Chicago, 2017.

[40] E. Tagliabue, "Visuo-haptic model of prostate cancer based on magnetic resonance elastography," University of Illinois at Chicago, 2017.

[41] C. Gatti, "Application of haptic virtual fixtures in psychomotor skill development for robotic surgical training," University of Illinois at Chicago, 2017.

[42] "Wykobi Computational Geometry Library." [Online]. Available: http://www.wykobi.com/. [Accessed: 15-Apr-2017].

[43] "Ascension Technology Corp." [Online]. Available: https://www.ascension-tech.com/. [Accessed: 15-Apr-2017].

[44] Paul Bourke, "Calculating Stereo Pairs." [Online]. Available: http://paulbourke.net/stereographics/stereorender/. [Accessed: 19-Nov-2017].

[45] M. Luisa, P. Salamanca, J. M. Sabater, M. Luisa, P. Salamanca, and J. M. Sabater, "Analysing collision detection in a virtual environment for haptic applications in surgery," vol. 31, no. 1, pp. 204–212, 2011.

[46] "GLUI User Interface Library." [Online]. Available: http://glui.sourceforge.net/. [Accessed: 13-Apr-2017].

[47] J. Brooke, "SUS - A quick and dirty usability scale," *Usability Eval. Ind.*, p. 189(194):4-7, 1996.

[48] A. Bangor, T. Staff, P. Kortum, J. Miller, and T. Staff, "Determining What Individual SUS Scores Mean : Adding an Adjective Rating Scale," vol. 4, no. 3, pp. 114–123, 2009.